USGS
science for a changing world

Prepared in cooperation with the State of Hawai‘i Commission on Water Resource Management

Identifying the Relative Importance of Water-Budget Information Needed to Quantify How Land-Cover Change Affects Recharge, Hawaiian Islands

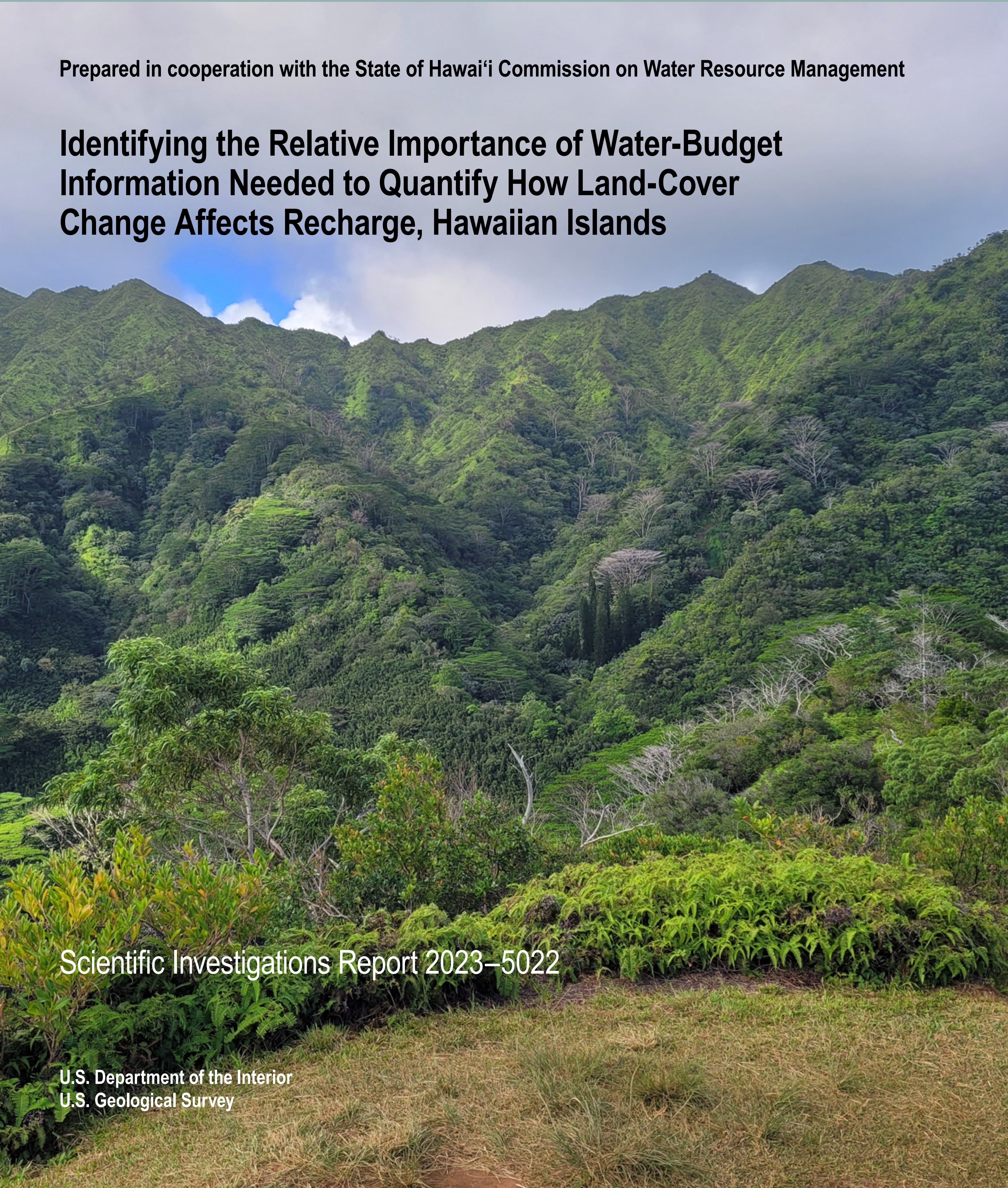

Scientific Investigations Report 2023–5022

U.S. Department of the Interior
U.S. Geological Survey

Cover. Photograph of Mānoa Valley uplands on the Island of Oʻahu, Hawaiʻi. U.S. Geological Survey photograph by Adam Johnson, June 2022.

Identifying the Relative Importance of Water-Budget Information Needed to Quantify How Land-Cover Change Affects Recharge, Hawaiian Islands

By Adam G. Johnson, Alan Mair, and Delwyn S. Oki

Prepared in cooperation with the State of Hawaiʻi Commission on
Water Resource Management

Scientific Investigations Report 2023–5022

U.S. Department of the Interior
U.S. Geological Survey

U.S. Geological Survey, Reston, Virginia: 2023

Suggested citation:
Johnson, A.G., Mair, A., and Oki, D.S., 2023, Identifying the relative importance of water-budget information needed to quantify how land-cover change affects recharge, Hawaiian Islands: U.S. Geological Survey Scientific Investigations Report 2023–5022, 28 p., https://doi.org/sir20235022.

Associated data for this publication:
Johnson, A.G., and Kāne, H.L., 2023, Model subareas and moisture zones used in a sensitivity analysis of a water-budget model completed in 2022 for the islands of Oahu and Maui, Hawaii: U.S. Geological Survey data release, https://doi.org/10.5066/P9X9ZEE3.

ISSN 2328-0328 (online)

Contents

Figures

Tables

Conversion Factors

U.S. customary units to International System of Units

Multiply	By	To obtain
	Length	
inch (in.)	2.54	centimeter (cm)
inch (in.)	25.4	millimeter (mm)
foot (ft)	0.3048	meter (m)
mile (mi)	1.609	kilometer (km)
	Area	
acre	4,047	square meter (m^2)
acre	0.4047	hectare (ha)
acre	0.4047	square hectometer (hm^2)
acre	0.004047	square kilometer (km^2)
square inch (in^2)	6.452	square centimeter (cm^2)
	Volume	
gallon (gal)	3.785	liter (L)
gallon (gal)	0.003785	cubic meter (m^3)
gallon (gal)	3.785	cubic decimeter (dm^3)
million gallons (Mgal)	3,785	cubic meter (m^3)
cubic inch (in^3)	16.39	cubic centimeter (cm^3)
	Flow rate	
gallon per day (gal/d)	0.003785	cubic meter per day (m^3/d)
million gallons per day (Mgal/d)	0.04381	cubic meter per second (m^3/s)
inch per year (in/yr)	25.4	millimeter per year (mm/yr)

Datum

Vertical coordinate information is referenced to local mean sea level.

Horizontal coordinate information is referenced to the North American Datum of 1983 (NAD 83).

Altitude, as used in this report, refers to distance above the vertical datum.

Abbreviations

AWC	available water capacity
CWRM	State of Hawai‘i Commission on Water Resource Management
DOFAW	State of Hawai‘i Division of Forestry and Wildlife
$\bar{E}/\bar{R}$	ratio of mean canopy evaporation rate during rainfall ($\bar{E}$) to mean precipitation rate ($\bar{R}$) for saturated canopy conditions
ET_o	reference-surface evapotranspiration
GIS	geographic information system
MDWS	County of Maui Department of Water Supply
NRCS	Natural Resources Conservation Service
OSDS	onsite sewage disposal system
PE	potential evapotranspiration
TMK	tax map key
TWIBH	trade wind inversion layer base height (altitude)
UHM	University of Hawai‘i at Mānoa
USGS	U.S. Geological Survey
WATRMod	Water-budget Accounting for Tropical Regions Model

Identifying the Relative Importance of Water-Budget Information Needed to Quantify How Land-Cover Change Affects Recharge, Hawaiian Islands

By Adam G. Johnson, Alan Mair, and Delwyn S. Oki

Abstract

Watershed management—the protection and restoration of native landscapes through a variety of actions—potentially can protect and improve groundwater availability by sustaining and enhancing groundwater recharge. The efficacy of watershed management for sustaining and enhancing groundwater recharge in the Hawaiian Islands, however, has not been quantified with certainty. A model that uses a water-budget approach—an accounting of the flow of water into and out of an area—is useful for assessing how regional-scale recharge for the Hawaiian Islands might be affected by land-cover changes associated with managed or unmanaged watersheds. However, the use of a water-budget model to confidently quantify how recharge might be affected by land-cover changes is impeded by uncertain values that model users assign to land-cover-dependent parameters. The parameter values, and thereby water-budget model recharge estimates, can likely be improved by the collection and analysis of additional hydrologic information.

This report describes a sensitivity analysis of a water-budget model that was completed to identify the most important types of hydrologic information needed to reduce the uncertainty of model recharge estimates. The sensitivity of model recharge estimates for the Hawaiian Islands of Oʻahu and Maui was analyzed for seven model parameters potentially affected by land-cover changes within a watershed. The seven model parameters tested were canopy capacity, canopy-cover fraction, crop coefficient, fog-catch efficiency, root depth, stemflow, and trunk-storage capacity.

Results of the sensitivity analysis were used to (1) quantify the relative importance of the seven model parameters to recharge assessments for three moisture zones (dry, mesic, and wet) on Oʻahu and Maui and (2) prepare a list of critical information needs for each moisture zone. The list of critical information needs was developed for three general types of land cover (forest, shrubland, and grassland) that are assumed to be affected by watershed management in the Hawaiian Islands. Identified information needs included estimates or measurements of (1) evapotranspiration processes needed to determine crop coefficients for land-cover types in all moisture zones, (2) rooting depths for land-cover types in the dry and mesic moisture zones, (3) canopy-cover fraction for forests in the wet and mesic moisture zones, (4) ratios of fog interception to rainfall for forests and shrublands in the wet moisture zone, and (5) canopy capacity for forests in the wet and mesic moisture zones. The list of information needs can guide data-collection strategies of future projects. Collection and analysis of the identified hydrologic information may help model users develop a better parameterization scheme, reduce uncertainty of values that model users assign to land-cover dependent parameters, and therefore allow future applications of the water-budget model to more accurately quantify how recharge in the Hawaiian Islands might be affected by future land-cover changes within a watershed.

Introduction

Groundwater is an important resource in the Hawaiian Islands. In 2010, groundwater provided 94 percent of all freshwater for public supply on the four islands (Oʻahu, Island of Hawaiʻi, Maui, and Kauaʻi) (fig. 1) that contain 99 percent of the State of Hawaiʻi's population (Izuka and others, 2018). Persistent discharge of groundwater to streams contributes to surface-water resources, which have aesthetic, cultural, ecologic, and economic importance (Oki and others, 2010).

Watershed management has the potential to protect and improve groundwater availability by sustaining and enhancing groundwater recharge. Watershed management in the Hawaiian Islands involves a variety of protection and restoration actions, including (1) removing feral ungulates (hooved animals such as pigs, goats, sheep, deer, and wild cattle) that can negatively affect forest ecosystems, (2) installing and maintaining fences around native forests and vegetation, (3) removing and containing nonnative invasive vegetation, (4) monitoring and controlling for the potential spread of wildfires, predators, plant diseases, and other threats to forests, (5) planting native vegetation, and (6) teaching residents and visitors about the cultural, economic, and environmental importance of conserving native forests (State of Hawaiʻi Department of Land and Natural Resources, 2011).

Watershed-management areas for Oʻahu and Maui include areas managed by five watershed partnerships (State of Hawaiʻi Department of Land and Natural Resources, 2018) (fig. 1) that are composed of public and private partners. The five watershed

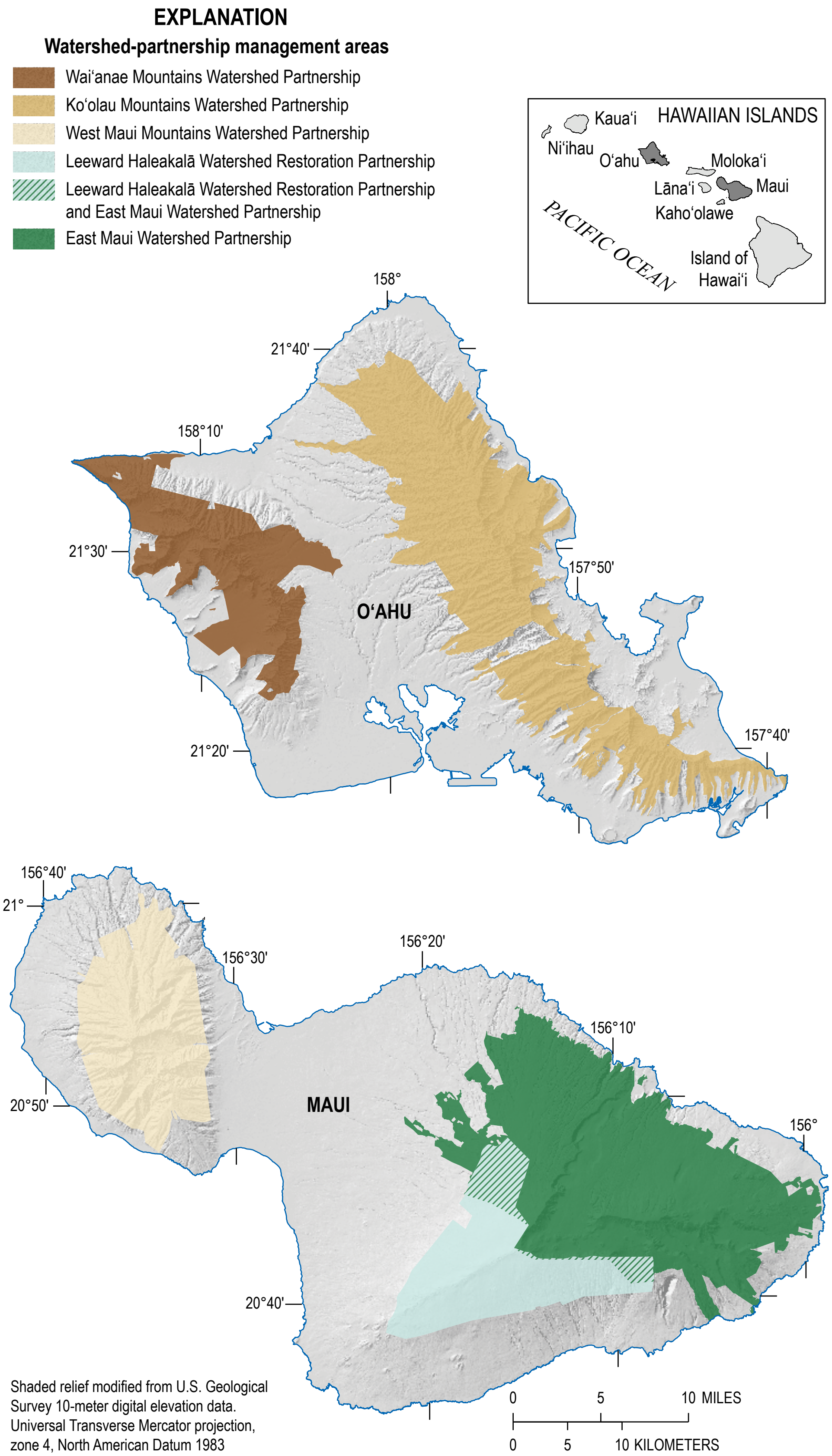

Figure 1. Maps showing areas managed by five watershed partnerships for the Islands of O‘ahu and Maui, Hawai‘i.

partnerships are Waiʻanae Mountains Watershed Partnership, Koʻolau Mountains Watershed Partnership, West Maui Mountains Watershed Partnership, Leeward Haleakalā Watershed Restoration Partnership, and the East Maui Watershed Partnership. About 39 percent of Oʻahu's total area and about 43 percent of Maui's total area are within the watershed-partnership management areas.

Background and Motivation

Although the spread of nonnative invasive forest species is purported to reduce fresh groundwater availability, the efficacy of watershed management for sustaining and enhancing groundwater recharge in the Hawaiian Islands has not been quantified with certainty. The lack of certainty is partly related to the fact that regional-scale recharge cannot be directly measured and must be estimated using indirect methods such as water-budget models.

In 2014, the County of Maui Department of Water Supply (MDWS), University of Hawaiʻi at Mānoa (UHM), and U.S. Geological Survey (USGS) Pacific Islands Water Science Center initiated a study to establish a framework for evaluating the hydrologic effects of watershed-management programs on Maui and Molokaʻi. With the support of additional collaborators including the State of Hawaiʻi Commission on Water Resource Management (CWRM) and the State of Hawaiʻi Division of Forestry and Wildlife (DOFAW), the scope of the study was expanded in 2016 and 2017 to include Kauaʻi, Oʻahu, and the Island of Hawaiʻi. The original objective of the study was to provide valuable information for (1) assessing effects of nonnative plant species on freshwater availability and (2) reducing uncertainty in regional recharge estimates from a water-budget model. The selection of model parameter values for high-priority species of concern, including both nonnative and native forest species, can be a source of uncertainty when information needed to estimate these values is lacking or insufficient. The study identified a need for an extensive field data-collection program that could acquire the types of information that model users need to estimate model parameter values for high-priority nonnative forest species of concern and dominant native forest species. The study conducted stakeholder workshops aimed, in part, at identifying high-priority nonnative plant species of concern, identifying dominant native forest plant species, as well as identifying and evaluating possible sites for field data collection. Several challenges associated with an extensive data-collection program were identified, including (1) an extended timeline for data collection, data analysis, and recharge estimation, (2) high data-collection costs, and (3) the need for guidance on the most relevant types of field data and where to collect these data. Therefore, to help guide future data-collection efforts, the study identified a need to further understand the sensitivity of model recharge estimates to select model parameters.

Models that use the water-budget approach are useful for quantifying how regional-scale recharge might be affected by land-cover changes within a watershed. The model developed by Oki (2022a)—Water-Budget Accounting for Tropical Regions Model (WATRMod)—uses the water-budget approach to estimate spatially distributed recharge and other water-budget components for islands in tropical settings. This water-budget model computes recharge according to equations written in the source code (Oki, 2022b) and model input files prepared by model users (hereafter shortened to "users"). WATRMod uses the equations and information from model input files to simulate hydrologic processes that affect recharge, including rainfall, fog interception, irrigation, septic-system leachate, runoff, and evapotranspiration. For the purpose of this report, "model input" includes any information in the model input files, whose format and content requirements are described by Oki (2022a). Model input includes (1) data, such as rainfall data and land-cover information for the area being modeled, (2) parameter values, which are numerical values assigned to parameters, such as root depth, in the model equations (Finch and Aronson, 1982), and (3) initial conditions at the start of a model simulation. For example, the land-cover input file contains land-cover-dependent parameter values that users assign to each unique land-cover class included in a study area.

WATRMod is a modified version of older models that were used to estimate spatially distributed mean annual recharge for several Hawaiian Islands for historical and recent climate conditions (Engott, 2011; Engott and others, 2017; Izuka and others, 2018; Johnson and others, 2018; Oki and others, 2020), for potential future climate conditions (Mair and others, 2019), and for potential future land-cover conditions (Brewington and others, 2019). Compared with older versions of the model used by the listed studies, WATRMod uses a similar water-budget approach and requires most of the same types of model input, but it uses an updated source code (Oki, 2022b) and contains more options for users (Oki, 2022a).

Use of models to confidently quantify how recharge for the Hawaiian Islands might be affected by managed or unmanaged watersheds is impeded by uncertainty in the parameter values that users assign to different types of land cover. For example, recent applications of water-budget models for Oʻahu and Maui assigned only one set of parameter values to each of the following types of land cover: (1) all types of grassland, (2) all types of shrubland, (3) all nonnative forests exposed to fog, (4) all nonnative forests not exposed to fog, and (5) all native forests (Engott and others, 2017; Brewington and others, 2019; Mair and others, 2019). This simplified parameterization scheme is imperfect and reflects the limited availability of relevant information that users had when estimating and assigning parameter values. Furthermore, this simplification may limit the model from accurately estimating how recharge might change in areas where existing vegetation is replaced by different species and types of grasses, shrubs, or nonnative trees. A better parameterization scheme could instead contain specific parameter values for different species of nonnative trees or additional types of forests such as native dry forest, native mesic forest, nonnative dry forest, and nonnative wet forest. The better parameterization scheme could allow models to properly simulate how different types of land cover affect groundwater recharge.

One challenge users may face when preparing model input is not knowing if or how much the parameter values for a given type of land cover, such as grassland, would differ between relatively dry and wet regions. For example, the recent applications of water-budget models for O‘ahu and Maui assigned a root depth of 39 inches (in.) to grassland land cover. Regional differences in grassland root depths were not accounted for in the model input, which may not have properly represented grassland root depths in the environment. Yang and others (2016) estimated effective rooting depths for global biomes, such as the grassland biome, and determined that the effective rooting depths for each biome have substantial spatial heterogeneity, which are related to spatial variability of climate. Therefore, for the Hawaiian Islands, variations in root depth (and possibly other land-cover dependent parameters) for each of the most widespread types of land cover could be substantial given the wide spatial ranges of mean annual rainfall (about 8 to 404 in. [Giambelluca and others, 2013]), and mean annual reference surface potential evapotranspiration (about 26 to 133 in. [Giambelluca and others, 2014]).

Brewington and others (2019) used an older version of the model to estimate mean annual groundwater recharge for Maui under four future land-cover scenarios and two future climate projections. They compared their results to baseline recharge that was estimated using 2017 land cover to understand how changing land management and climate could influence groundwater recharge. Their analyses suggested that potential changes in future land cover could increase island-wide mean annual groundwater recharge rates by as much as 10 percent for a wet-climate scenario and 12 percent for a dry-climate scenario. However, they also noted that a lack of data or a sparse, uneven distribution of data in space and time, coupled with a poor understanding of some hydrologically relevant processes, could limit the precision and accuracy of model recharge estimates. For example, the differences in transpiration rates of native and nonnative forest species in the Hawaiian Islands are not well known. As a result, Brewington and others (2019) were only able to distinguish three types of forested land cover: native forest, nonnative forest, and tree plantation.

Collection and analysis of additional hydrologic information may not only help users develop a better parameterization scheme but also reduce the uncertainty of values that users assign to land-cover-dependent model parameters and, therefore, allow future applications of the model to accurately quantify how recharge might be affected by land-cover changes within a watershed. Collection and analysis of hydrologic information, however, can be expensive and time consuming, especially for collection of multiple types of data across multiple regions. Some types of data may be more important than others in terms of reducing uncertainty of model recharge estimates. To improve the efficiency of data collection, analysis is needed to identify the most beneficial hydrologic information to collect in different regions in the Hawaiian Islands.

Purpose and Scope

The purpose of this report is to describe a study that identified and summarized the types of hydrologic information that are critical for quantifying how recharge for the Hawaiian Islands might be affected by managed or unmanaged watersheds. The study used WATRMod (Oki, 2022a), which was designed to estimate spatially distributed recharge and other water-budget components for tropical islands. The study completed a sensitivity analysis of WATRMod to evaluate the sensitivity of modeled recharge estimates to seven parameters that might be affected by land-cover changes within a watershed. The selected model parameters were canopy capacity, canopy-cover fraction, crop coefficient, fog-catch efficiency, root depth, stemflow, and trunk-storage capacity (table 1). The scope of the sensitivity analysis was limited to a simple, one-at-a-time approach (Hamby, 1994) in which one parameter value was varied while the remaining parameters were held fixed at baseline values. Results of the sensitivity analysis were used to determine the relative importance of each parameter in estimating recharge for the three moisture zones (dry, mesic, and wet) defined by Price and others (2012) for the Hawaiian Islands (fig. 2). The scope of the sensitivity analysis was limited to the islands of O‘ahu and Maui. The scope of the study did not include prediction of future land-cover conditions or estimation of recharge for future land-cover conditions.

Sensitivity Analysis

The sensitivity of modeled mean annual recharge estimates for O‘ahu and Maui was evaluated for the following seven model parameters potentially affected by land-cover change associated with watershed management: canopy capacity, canopy-cover fraction, crop coefficient, fog-catch efficiency, root depth, stemflow, and trunk-storage capacity (table 1).

Four of the seven model parameters (canopy capacity, canopy-cover fraction, stemflow, and trunk-storage capacity) are used by the model to compute canopy evaporation for forests, using the Gash and others (1995) sparse-forest approach. Canopy capacity, expressed as depth per unit area of cover (Gash and others, 1995), represents the maximum amount of water left on the canopy in zero evaporation conditions after precipitation and throughfall ceased (Gash and Morton, 1978). Stemflow and trunk-storage capacity are used by the model to estimate tree-trunk evaporation, which is included in the model estimates of canopy evaporation.

A crop coefficient is an empirically derived ratio of potential evapotranspiration (*PE*) for a certain type of land cover to reference evapotranspiration (ET_o). The parameter, ET_o, is derived from meteorological data using the Food and Agricultural Organization Penman-Monteith method and represents the evapotranspiration rate from a hypothetical reference surface with a particular height, surface resistance, and albedo for the prevailing climatic conditions (Allen and others, 1998). The reference surface resembles a green, well-watered grass surface of uniform height

Table 1. Model parameters potentially affected by land-cover change and evaluated in a sensitivity analysis of a water-budget model for the Islands of Oʻahu and Maui, Hawaiʻi.

Model parameter	Explanation [dimension]	Hydrologic condition or process simulated by model using assigned parameter values	Source(s) of data, analyses, and assumptions used to determine baseline values for grassland, forest, and shrubland types of land cover
Canopy capacity	Water-retention capacity of forest canopy per unit area of cover [length]	Canopy evaporation	DeLay (2005), Takahashi and others (2011), Safeeq and Fares (2014), Engott and others (2017)
Canopy-cover fraction	Fraction of ground area covered by forest canopy [dimensionless]	Canopy evaporation	Giambelluca and others (2014)
Crop coefficient	Scaling coefficient for reference evapotranspiration that is dependent on the type of land cover [dimensionless]	Potential evapotranspiration	Allen and others (1998), Engott and others (2017)
Fog-catch efficiency	Represents fog-collecting ability of vegetation expressed as a fraction of the reference fog-catch efficiency assigned to forested land covers [dimensionless]	Fog interception	Engott (2011)
Stemflow	Fraction of precipitation diverted to stemflow once canopy is saturated [dimensionless]	Canopy evaporation	Gaskill (2004), DeLay, (2005), Takahashi and others (2011), Safeeq and Fares (2014), Engott and others (2017)
Root depth	Average root depth of vegetation for an area [length]	Soil-moisture storage capacity; actual evapotranspiration	Allen and others (1998), Engott (2011), Fares (2013), Engott and others (2017)
Trunk-storage capacity	Water-retention capacity of trunks [length]	Canopy evaporation	DeLay (2005), Safeeq and Fares (2014), Engott and others (2017)

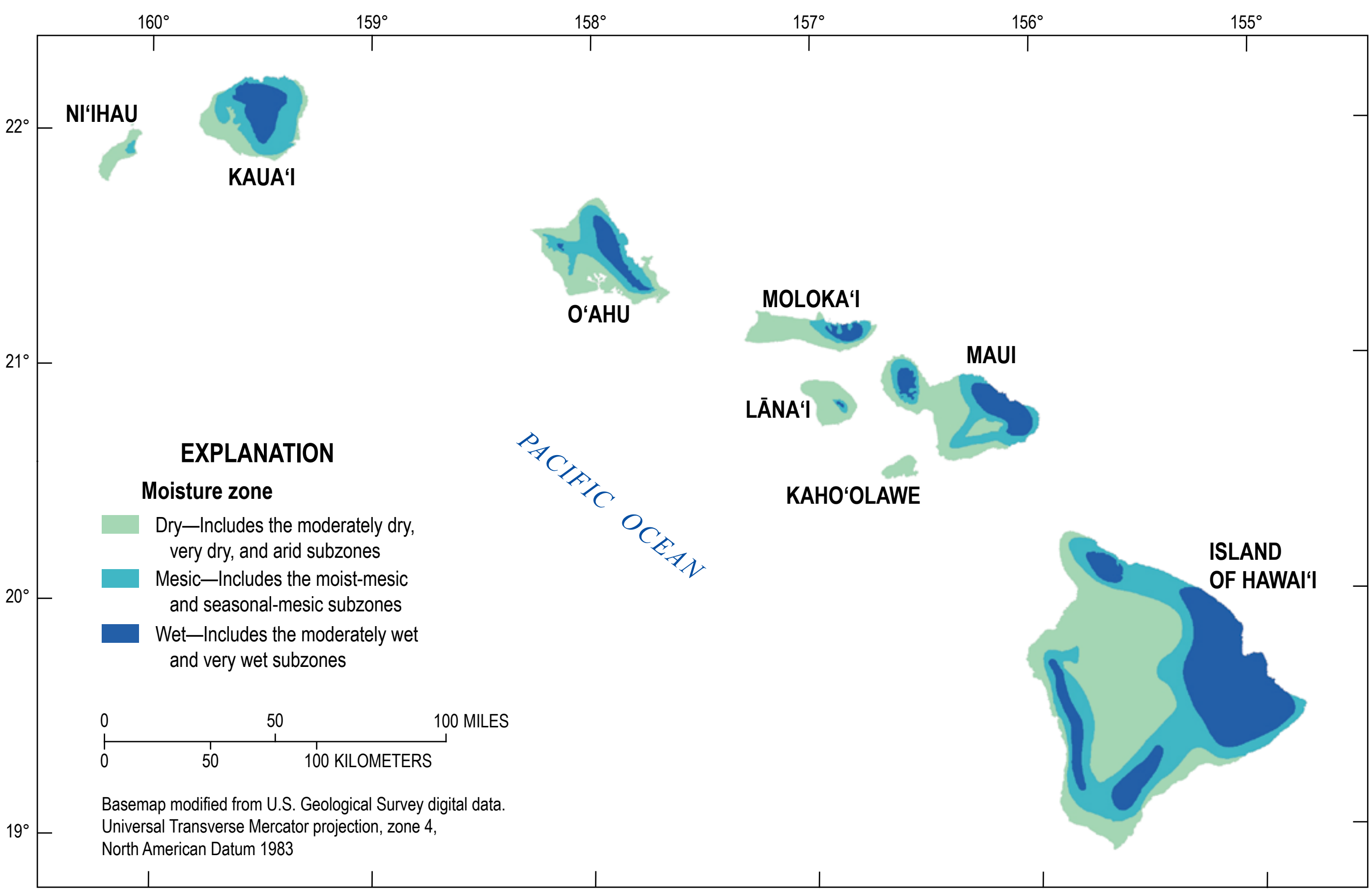

Figure 2. Map of the Hawaiian Islands showing moisture zones. Modified from Price and Jacobi (2012) and Price and others (2012).

and that completely shades the ground. The model calculates *PE* for a particular area as the product of ET_o and the crop coefficient assigned to the area's land-cover type. The term "crop coefficient" can be misleading because the model uses crop coefficient to calculate *PE* for all areas, including areas with nonagricultural types of land cover, such as native forest. The utility of the crop-coefficient parameter might be more easily understood if the parameter is thought of as an "evapotranspiration coefficient" or "land-cover coefficient." The parameter is referred to as "crop coefficient" in this report for the purpose of consistency with the model documentation (Oki, 2022b).

Fog-catch efficiency is used in the model computation of fog interception, which represents cloud water that is intercepted by vegetation. Intercepted cloud water that does not evaporate ultimately reaches the ground as the fog-drip component of net precipitation and contributes moisture to the plant-root zone. The model uses fog-catch efficiency values, which are expressed as a fraction of the reference fog-catch efficiency value assigned to a reference land-cover type, to account for differences in the fog-collecting ability of land-cover types for prevailing fog conditions. In recent applications of previous model versions, forest land covers were the reference land cover and were assigned a fog-catch efficiency of 1 (Engott, 2011; Engott and others, 2017; Izuka and others, 2018; Mair and others, 2019; Oki and others, 2020). In areas with no fog, however, fog-catch efficiency does not affect recharge estimates.

Root depth is the average rooting depth of vegetation represented by a type of land cover. The model multiplies root depth by soil-available water capacity to compute the moisture-storage capacity of the plant-root zone, where soil-available water capacity is the quantity of water that the soil is capable of storing for use by plants (Natural Resources Conservation Service [NRCS], 2019a, b).

The model allows users to assign values that vary spatially to many parameters, including all seven parameters evaluated in the sensitivity analysis. For example, users typically assign values to the crop-coefficient parameter by land-cover type, which usually varies spatially within a study area. Therefore, one might consider crop coefficient to be a "parameter group" instead of a "parameter" because different land-cover types usually are assigned different crop-coefficient values. The authors of this report, however, opted to use "parameter" because it is a simpler term than "parameter group."

The sensitivity analysis did not evaluate model inputs that are assumed to be mostly unaffected by watershed management. Model input not evaluated in the sensitivity analysis included monthly rainfall, daily-to-monthly rainfall ratios, monthly fog-to-rainfall ratios, monthly ET_o, soil available water capacity, irrigation efficiency, irrigation multiplier, the supply-based irrigation rate for taro, direct-recharge rates, and septic-leachate rates. Monthly runoff-to-rainfall ratios, which are model inputs that can be affected by land-cover change, were not evaluated in the sensitivity analysis because the effect of land-cover change on runoff has not been measured for watersheds in Hawai‘i. Information used to prepare these model-input components for the sensitivity analysis is described in this report (see "Model Input Not Evaluated" section). Oki (2022a) provided descriptions of all model input required for the model.

General Approach of Sensitivity Analysis

Using a one-at-a-time approach (Hamby, 1994), this study evaluated the sensitivity of mean annual recharge (hereafter, recharge) estimates from WATRMod to seven model parameters (table 1). WATRMod was used to estimate spatially distributed recharge for O‘ahu and Maui for a baseline scenario and 42 sensitivity scenarios (six scenarios for each of the seven parameters). For the baseline scenario, the seven model parameters were assigned baseline values (table 2) that were similar to the values used in recent recharge assessments by Engott and others (2017) and Mair and others (2019) (see "Model Input" section). In contrast, each sensitivity scenario used a unique set of modified baseline values for the seven model parameters and therefore represented a unique location in parameter space (table 3). The components of model input that were not evaluated in the sensitivity analysis were the same for every scenario. The model output for each scenario included recharge estimates for subareas of O‘ahu and Maui. The parameter values and subarea recharge estimates were used to compute 21 sensitivity indices, one for each parameter (table 3) and each moisture zone (dry, mesic, and wet) (fig. 2). A parameter's sensitivity index for a moisture zone characterizes the relation between the parameter's values and model recharge estimates for the zone (see "Computation of Parameter Sensitivity Indices for Moisture Zones" section). Sensitivity indices were used to quantify the relative importance of the seven parameters to model recharge estimates for the three moisture zones.

The model scenarios tested a range of plausible values for each of the seven selected parameters. The values tested for each selected parameter are described in this report (table 3) as percentages of the parameter's baseline values. Values tested for canopy-cover fraction ranged from 40 to 100 percent of the baseline values. The canopy-cover fraction values tested in the model scenarios did not exceed baseline values because (1) the model does not allow canopy-cover fraction values to exceed 1 and (2) substantial areas with forest on O‘ahu and Maui had baseline canopy-cover fraction values that were near 1. For example, the baseline canopy-cover fraction was greater than 0.90 for approximately half of the combined forest area on O‘ahu and Maui.

Crop coefficients tested in the sensitivity scenarios varied between 0.20 and 1.40, which represents the general range of crop coefficients reported by Allen and others (1998) for dozens of different types of crops and vegetation. For each type of land cover (table 2), interim crop coefficients were 40, 60, 80, 120, 160, and 200 percent of the baseline crop-coefficient value(s). Each crop coefficient used in the sensitivity scenarios was (1) equal to its interim value if its interim value was between 0.20 and 1.40, (2) set to 0.20 if its interim value was less than 0.20, and (3) set to 1.40 if its interim value was greater than 1.40.

Table 2. Baseline values assigned to six of seven parameters evaluated in a sensitivity analysis of a water-budget model for the Islands of Oʻahu and Maui, Hawaiʻi.

[Percentage of island area determined from land-cover maps for Oʻahu (modified from Engott, 2017) and Maui (modified from Mair, 2018). Baseline values for canopy-cover fraction varied spatially and were determined from spatial estimates of vegetation-cover fraction (Giambelluca and others, 2014). Abbreviations: --, land-cover type not included in island's land-cover map; in., inch]

Land-cover type(s)	Forest or nonforest	Percentage of island area		Baseline parameter values					
		Maui	Oʻahu	Canopy capacity (in.)	Crop coefficient	Fog-catch efficiency	Root depth (in.)	Stemflow, fraction of precipitation	Trunk-storage capacity (in.)
Grassland[1]	Nonforest	33.9	8.2	0.00	0.95	0.0	39	0.00	0.00
Native forest[2]	Forest	20.1	16.1	0.05	0.30	1.0	30	0.04	0.01
Nonnative forest[3]	Forest	14.7	24.2	0.05	[4]0.33, [5]0.44	1.0	60	0.04	0.01
Shrubland	Nonforest	8.6	13.0	0.00	1.00	0.5	12	0.00	0.00
Sparsely vegetated	Nonforest	5.9	0.6	0.00	1.18	0.0	5	0.00	0.00
Developed, open space	Nonforest	5.1	--	0.00	1.18	0.0	12	0.00	0.00
Kiawe/phreatophytes	Forest	4.8	1.2	0.05	0.84	1.0	71	0.04	0.01
Developed, low intensity	Nonforest	2.8	14.8	0.00	1.18	0.0	12	0.00	0.00
Developed, medium intensity	Nonforest	1.2	7.4	0.00	1.18	0.0	12	0.00	0.00
Developed, high intensity	Nonforest	0.8	5.6	0.00	1.18	0.0	12	0.00	0.00
Tree plantation[6]	Forest	0.5	2.1	0.05	[4]0.33, [5]0.44	1.0	60	0.04	0.01
Diversified agriculture	Nonforest	0.4	2.8	0.00	1.00	0.0	10	0.00	0.00
Golf course	Nonforest	0.4	1.4	0.00	0.85	0.0	30	0.00	0.00
Pineapple	Nonforest	0.3	0.7	0.00	0.30	0.0	18	0.00	0.00
Seed corn	Nonforest	0.2	0.9	0.00	[7]0.29–1.20	0.0	18	0.00	0.00
All water bodies and reservoirs	Nonforest	0.2	0.7	0.00	1.05	0.0	1	0.00	0.00
Coffee	Nonforest	0.1	<0.1	0.00	0.91	0.5	48	0.00	0.00
Macadamia	Nonforest	<0.1	<0.1	0.00	0.91	1.0	60	0.00	0.00
Taro	Nonforest	<0.1	<0.1	0.00	1.25	0.0	15	0.00	0.00
Wetland	Nonforest	<0.1	0.3	0.00	1.18	0.0	39	0.00	0.00

[1]Includes two land-cover types (grassland and fallow/grassland) from land-cover maps.

[2]Includes three land-cover types (native forest; native forest, fog; and native forest, no fog) from land-cover maps.

[3]Includes three land-cover types (alien forest; alien forest, fog; and alien forest, no fog) from land-cover maps.

[4]Crop coefficient assigned to nonnative forest and tree plantation within and above cloud zone.

[5]Crop coefficient assigned to nonnative forest and tree plantation below cloud zone.

[6]Includes three land-cover types (tree plantation; tree plantation, fog; and tree plantation, no fog) from land-cover maps.

[7]Crop coefficients for seed corn varied by month: Jan. and July, 0.85; Feb. and Aug., 0.50; Mar. and Sept., 0.29; Apr. and Oct., 0.40; May and Nov. 0.80; June and Dec., 1.20.

The range of values tested for canopy capacity (0.01–0.15 in.), stemflow (0.02–0.30 fractional units of precipitation during saturated canopy conditions), and trunk-storage capacity (0.01 to 0.06 in.) were considered plausible because they were within the ranges of mean values estimated for forest sites in the Hawaiian Islands (see, for example, Gaskill, 2004; DeLay, 2005; Mair and Fares, 2010; Giambelluca and others, 2011; Takahashi and others, 2011; Safeeq and Fares, 2014). In terms of percentages of baseline values, the range of values tested for canopy capacity (60–300 percent), stemflow (50–750 percent), and trunk-storage capacity (40–600 percent) were wider than ranges of values tested for the other four parameters (table 3) because baseline values for canopy capacity, stemflow, and trunk-storage capacity were small (table 2). Values tested for root depths were between 40 and 200 percent of baseline values and were considered plausible because they were within the range of global root-depth estimates for biomes and lifeforms (Schenk and Jackson, 2002; Yang and others, 2016).

The fog-catch efficiency parameter is used as a surrogate in the sensitivity analysis for fog interception, which is a hydrologic process represented in the model (fig. 3). The reason for using fog-catch efficiency instead of fog interception is because the spatial and temporal distribution of fog interception across the Hawaiian Islands is uncertain. Consequently, the values that users assign to parameters (fog-catch efficiency and fog-to-rainfall ratio) within WATRMod to compute fog interception are uncertain and, therefore, the model's fog-interception estimates are uncertain. Because the model's fog interception estimates are directly proportional to fog-catch efficiency and fog-to-rainfall ratio, the authors' choice to include only one of these parameters (fog-catch efficiency) in the sensitivity analysis is a simplified yet adequate approach for evaluating the sensitivity of model recharge estimates

Table 3. Summary of parameter values assessed in model scenarios completed for a sensitivity analysis of a water-budget model for the Islands of O‘ahu and Maui, Hawai‘i.

[Baseline values for canopy capacity, crop coefficient, fog-catch efficiency, root depth, stemflow, and trunk-storage capacity varied by land-cover type (table 2). Baseline values for canopy-cover fraction varied spatially and were determined from spatial estimates of vegetation-cover fraction (Giambelluca and others, 2014). Abbreviations: CE, canopy evaporation; ET, evapotranspiration; SE, soil evaporation; T, transpiration]

Parameter	Parameter values assessed in model scenarios	Application in model scenarios for sensitivity analysis
Canopy capacity	60, 100, 140, 180, 220, 260, and 300 percent of baseline values	Greater than zero for forest land-cover types only
Canopy-cover fraction	40, 50, 60, 70, 80, 90, and 100 percent of baseline values	Greater than zero for forest land-cover types only
Crop coefficient	40, 60, 80, 100, 120, 160, and 200 percent of baseline values, but no less than 0.20 and no greater than 1.40	Used to estimate potential rate of SE and T combined for forest land-cover types; used to estimate potential rate of total ET (CE, SE, and T combined) for nonforest land-cover types
Fog-catch efficiency	40, 60, 80, 100, 120, 160, and 200 percent of baseline values	Greater than zero for land-cover types with relatively tall vegetation (trees, shrubs, and coffee) only
Root depth	40, 60, 80, 100, 120, 160, and 200 percent of baseline values	Greater than zero for all land-cover types
Stemflow	50, 100, 150, 200, 250, 350, and 750 percent of baseline values	Greater than zero for forest land-cover types only
Trunk-storage capacity	40, 100, 200, 300, 400, 500, and 600 percent of baseline values	Greater than zero for forest land-cover types only

to fog interception. Testing fog-catch efficiency values that differed from the baseline fog-catch efficiency values can be considered analogous to the testing of fog-to-rainfall ratios that differed from baseline fog-to-rainfall ratios.

The modeled sensitivity scenarios included those that tested fog-catch efficiency values of 1.2, 1.6, and 2 for forest land-cover types. Scenarios that tested fog-catch efficiency values that exceeded the upper end of the range (0 to 1) described in WATRMod’s documentation (Oki, 2022a) were included and assumed to represent plausible conditions because the spatial distribution of fog interception for the Hawaiian Islands is uncertain. Furthermore, the baseline area-weighted average fog-interception estimates for windward forests and leeward forests were conservative relative to fog-interception estimates that were derived from field measurements at multiple forested locations in the Hawaiian Islands (see, for example, DeLay and Giambelluca, 2010; Giambelluca and others, 2011; Juvik and others, 2011; Takahashi and others, 2011). Because fog-catch efficiency was a surrogate for fog interception in the sensitivity analysis, the scenarios that tested fog-catch efficiency values greater than the baseline values were used to quantify changes in recharge when fog-interception values were greater than the baseline fog-interception values.

Model Used to Estimate Spatially Distributed Recharge

WATRMod uses a water-budget approach in which recharge is assumed to occur when water in the plant-root zone (fig. 3) exceeds the soil’s moisture storage capacity (Oki, 2022a). WATRMod accounts for daily inputs of water to the plant-soil system (precipitation [which consists of rainfall and fog interception], irrigation, and septic-system leachate) and estimates daily outputs of water (runoff, evapotranspiration, and recharge). The plant-soil system consists of the exposed vegetation (for example, the forest canopy and tree trunks), built surfaces, and soil and water within the plant-root zone (fig. 3). WATRMod can also account for other sources of water, including direct recharge, which represents processes such as cesspool seepage that bypass the plant-root zone. Details of WATRMod, including descriptions of model inputs and outputs, are presented by Oki (2022a).

Model Subareas

WATRMod is designed to simulate hydrologic processes and compute recharge for subareas of the overall study area (Oki, 2022a). A map of the subareas is analogous to a model feature commonly referred to as a model grid. Each subarea can be an irregularly shaped area of nonuniform size or a regular gridded area of uniform size. The boundaries and spatial extents of the subareas are defined by the user prior to executing the model. Subareas can be defined by overlaying (intersecting) geographic information system (GIS) datasets that contain spatially variable model-input information, such as grid cells used to estimate monthly rainfall and polygons representing land-cover types (see, for example, fig. 2 of Oki, 2022a). The subareas are hydrologically independent, meaning that WATRMod does not route runoff or water from one subarea to an adjacent subarea, although WATRMod does have the capability to incorporate subarea-specific runoff estimates that account for such routing. WATRMod

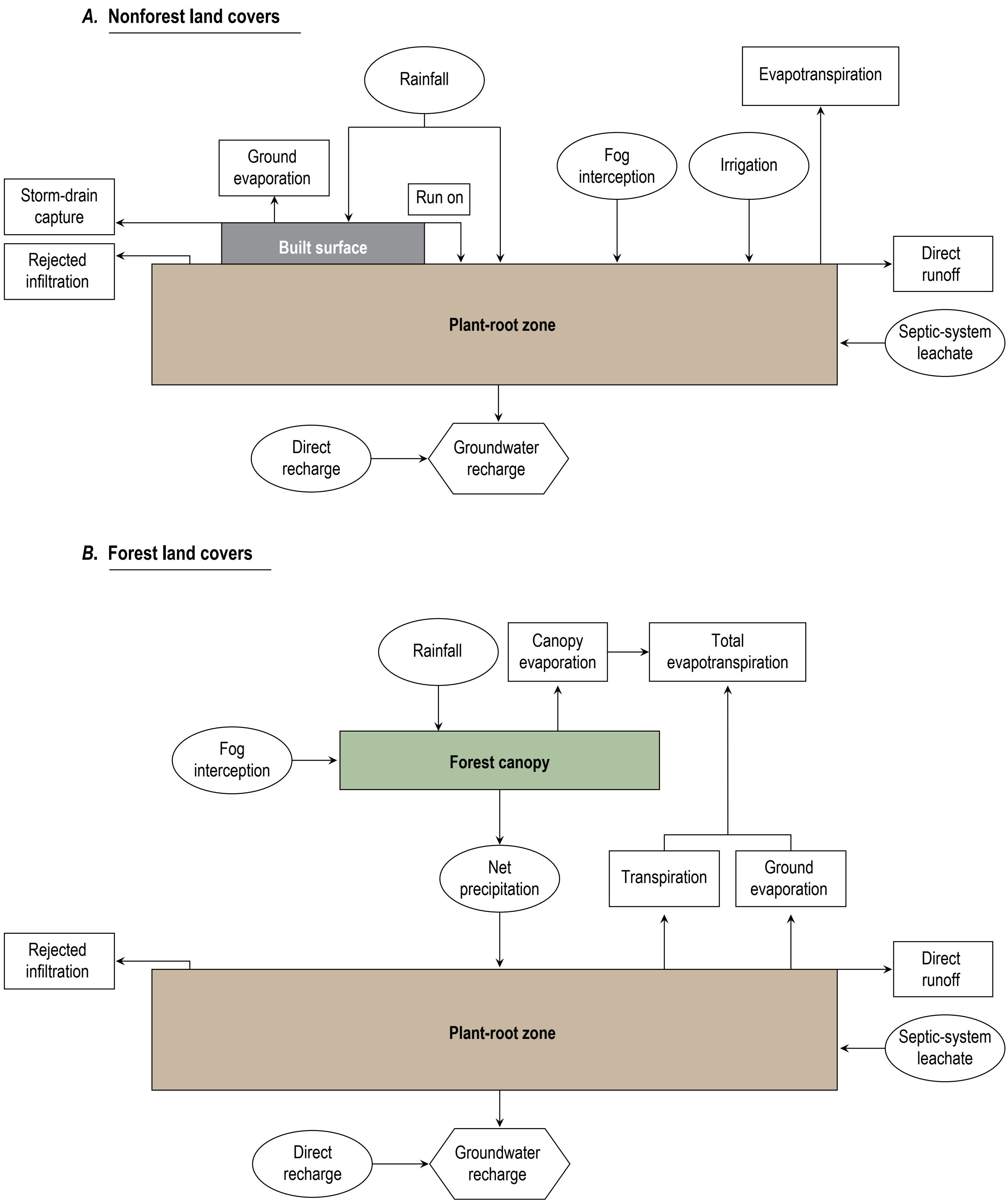

Figure 3. Conceptual water-budget flow diagrams for nonforest (*A*) and forest (*B*) land covers. Forest land-cover flow diagram modified from McJannet and others (2007).

requires a subarea-specific input file with information for each subarea such as its land-cover type. The model output includes recharge estimates for the subareas and aggregated recharge values for larger areas, such as the overall study area.

The authors generated a map of subareas for the islands of Oʻahu and Maui for the purpose of preparing model input used in the sensitivity analysis (Johnson and Kāne, 2023). Subarea maps for both islands were generated in a GIS program by intersecting spatial datasets used to characterize the spatial distribution of rainfall, fog interception, ET_o, runoff, soil properties, land cover, and wastewater discharge from onsite sewage disposal systems (OSDSs). The subarea maps were used to create the subarea-specific model input file for each island, which requires a specific format and set of attributes that are described by Oki (2022a). The spatial datasets used to create the subarea maps cannot be read by the model and therefore are not model input.

Spatial datasets that were merged to create the map of model subareas for Oʻahu included maps of

1. Grid cells for the Rainfall Atlas of Hawaiʻi (Giambelluca and others, 2013) and Evapotranspiration Atlas of Hawaiʻi (Giambelluca and others, 2014),
2. Tax-map key (TMK) parcels identified by Hawaiʻi State Department of Health (2017) as having OSDSs,
3. Aspect and runoff zones (Engott and others, 2017),
4. Soil units (NRCS, 2019b),
5. Recent land cover (Engott, 2017), and
6. Areas below and within the cloud zone (fig. 4).

For Oʻahu—which has a maximum altitude of 4,025 feet (ft)—all areas at or above 2,000 ft were assumed to be within the cloud zone and all areas below 2,000 ft were assumed to be below the cloud zone (fig. 4); this assumption is consistent with Engott and others (2017). For this study, the Oʻahu subarea map contained 342,654 subareas with an average area of 1.1 acres (4,517 square meters).

Spatial datasets that were merged to create the map of model subareas for Maui included maps of

1. Grid cells for the Rainfall Atlas of Hawaiʻi (Giambelluca and others, 2013) and Evapotranspiration Atlas of Hawaiʻi (Giambelluca and others, 2014),
2. TMK parcels identified by Hawaiʻi State Department of Health (2017) as having OSDSs,
3. Aspect and runoff zones (Johnson and others, 2018),
4. Soil units (NRCS, 2019a),
5. Recent land cover, and
6. Areas below, within, and above the cloud zone (fig. 4).

The recent land-cover map for Maui was the same as a 2017 land-cover map (Mair, 2018), except that it included one additional land-cover type, kiawe/phreatophytes, whose spatial extent was determined from the "Kiawe forest and Shrubland" class in a separate land-cover map (National Gap Analysis Program, 2011). The Maui subarea map consisted of 374,956 subareas with an average area of 1.2 acres (5,028 square meters).

For Maui, the base altitude of the cloud zone for windward areas was assumed to be 2,000 ft (fig. 4), consistent with the assumptions of Johnson and others (2018) and Mair and others (2019). The base altitude of the cloud zone for leeward areas was assumed to be 2,600 ft because Juvik and Hughes (1997) described an absence of fog below 2,600 ft and the presence of fog above that altitude for leeward areas on eastern Maui. Based on radiosonde observations for two sites—one on Kauaʻi and one on the Island of Hawaiʻi—during wet weather conditions between 1998 and 2011, Zhang and others (2012) estimated a mean trade wind inversion layer base height (TWIBH) of 7,480 ft for the Kauaʻi site and 8,038 ft for the Island of Hawaiʻi site. The nearest 100-ft altitude contour to the average of the TWIBH altitudes was 7,800 ft, which was the assumed top altitude of the cloud zone for leeward and windward areas in this study. Zhang and others (2012) also estimated mean TWIBH altitudes for the same sites during dry conditions, but the mean TWIBH altitudes during dry conditions were not considered in this study. Instead, only the mean TWIBH altitudes during wet conditions were selected because wet conditions were assumed to be most representative of conditions when fog interception occurred, given that WATRMod estimates fog interception using fog-to-rainfall ratios.

Model Input

Each scenario included in the sensitivity analyses used a unique set of model input files (table 3). Model input for the baseline scenario contained baseline values for all seven selected parameters that were evaluated in the sensitivity analysis. The baseline values for each parameter (table 2) are represented in table 3 as 100 percent of baseline values. The model input for each sensitivity scenario included a set of modified baseline values (table 3) for only one of the selected parameters and contained baseline values (table 2) for the other six selected parameters. The components of model input that were not evaluated in the sensitivity analysis were the same for every scenario.

Baseline Values for Seven Selected Model Parameters

Each subarea (Johnson and Kāne, 2023) was assigned one baseline value for each of the seven parameters that was included in the sensitivity analysis. The baseline canopy-cover fractions that were assigned to subareas were determined from a map of gridded estimates of vegetation-cover fraction obtained from Giambelluca and others (2014) and University of Hawaiʻi (2014b). The baseline values for the remaining six parameters evaluated in the sensitivity analysis were assigned to subareas according to their land-cover type (table 2) and generally were the same as the baseline values used in recent applications of previous versions of the model for Oʻahu and Maui (Engott and others, 2017; Mair and others, 2019). For taro land cover, however, baseline values assigned to root depth (15 inches) and crop coefficient (1.25) were equal to the averages of the root depths and crop coefficients specified for wetland taro by Fares (2013).

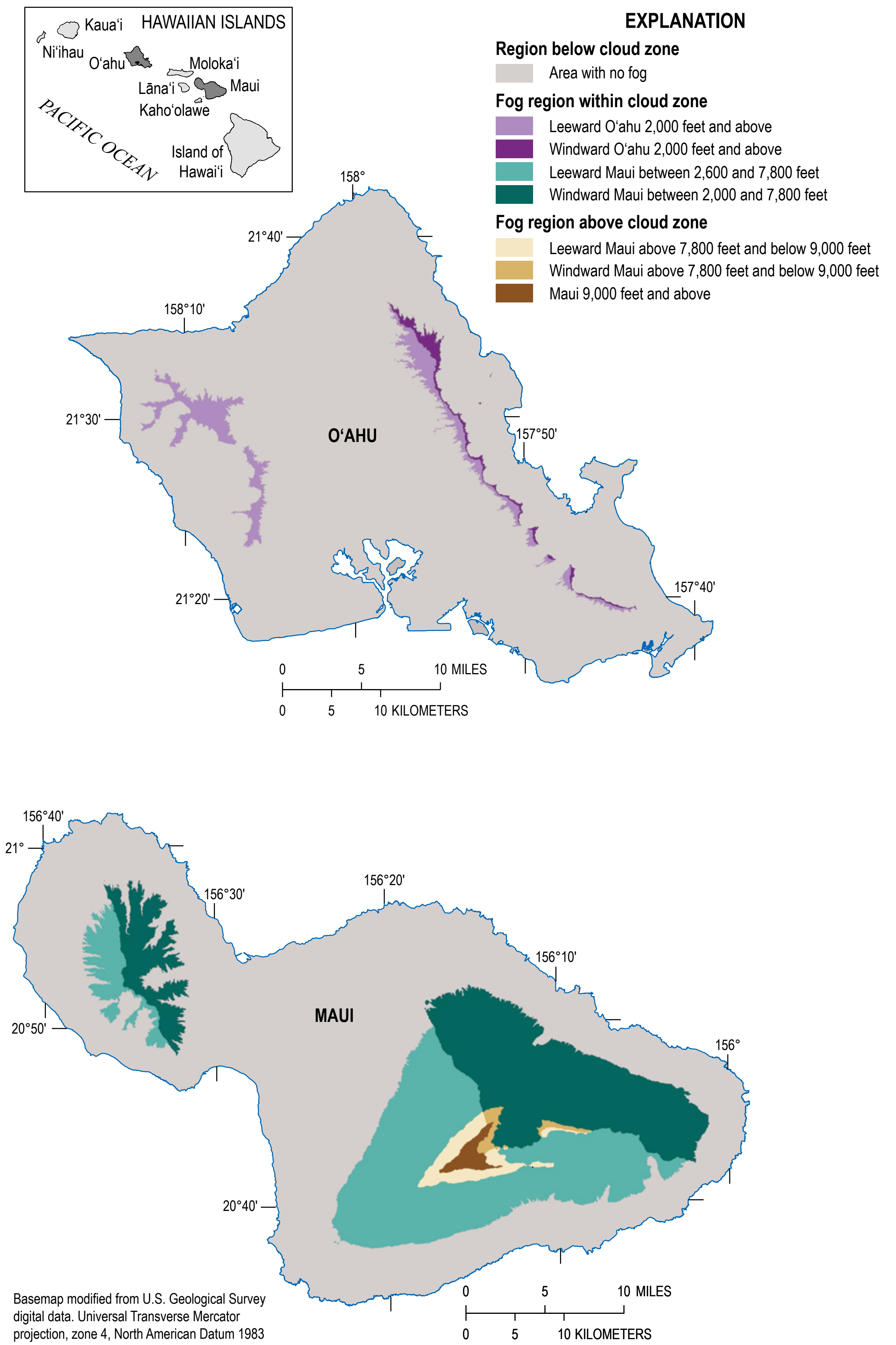

Figure 4. Maps showing cloud zone and fog regions for the Islands of O'ahu and Maui, Hawai'i.

Crop coefficients assigned to nonforest land-cover types were assumed to integrate the effects of transpiration, ground evaporation, and canopy evaporation. Crop coefficients assigned to forest land-cover types were assumed to integrate the effects of transpiration and ground evaporation only because canopy evaporation was accounted for separately (fig. 3; table 3). The same assumptions were made by recent applications of previous versions of the model for Oʻahu and Maui (Engott and others, 2017; Mair and others, 2019).

Model Input Not Evaluated

The components of model input that were not evaluated in the sensitivity analysis were the same for every scenario and generally were the same as or similar to model input used in recent applications of previous versions of the model by (1) Engott and others (2017) for Oʻahu for 1978–2007 climate conditions and (2) Mair and others (2019) for Maui for 1978–2007 conditions. Model input for this study that differed from what was used in these recent studies either incorporated new information or accounted for updates to model-input requirements, or both.

All scenarios simulated rainfall for the 30-year period (1978–2007) used by the Rainfall Atlas of Hawaiʻi (Giambelluca and others, 2013). Monthly rainfall estimates during 1978–2007 for each rainfall grid cell (about 770 by 820 ft) on Maui and Oʻahu were obtained from University of Hawaiʻi (2015) and Frazier and others (2016). In the model calculations, monthly rainfall values were multiplied by mean monthly adjustment factors (Engott and others, 2017; Johnson and others, 2018) so that mean monthly rainfall computed by WATRMod would match that estimated by Giambelluca and others (2013). WATRMod disaggregated adjusted monthly rainfall into daily rainfall using the method described by Oki (2022a) and monthly sets of daily-to-monthly rainfall ratios that were randomly selected by the model. Sets of daily-to-monthly rainfall ratios for each calendar month were prepared for each rainfall grid cell using gridded estimates of daily rainfall for 1990–2014 (Longman and others, 2019). Daily-to-monthly rainfall ratios for a particular month and rainfall grid cell were computed as ratios of daily rainfall to the sum of daily rainfall for the month. Thus, the sum of daily-to-monthly rainfall ratios in a set equaled 1, which ensured that adjusted monthly rainfall values derived from Frazier and others (2016) were preserved in the model calculations. Monthly runoff-to-rainfall ratios for runoff zones on Oʻahu and Maui were computed for 1978–2007 using the method described by Mair and others (2019).

Estimates of fog-to-rainfall ratios were needed for the model scenarios because WATRMod computed daily fog interception as the product of daily rainfall, a fog-to-rainfall ratio, and a fog-catch efficiency value (table 2). Fog-to-rainfall ratios for a given day were assumed to equal mean monthly fog-to-rainfall ratios for the corresponding month. For Oʻahu, mean monthly fog-to-rainfall ratios determined by Engott and others (2017) were used for all scenarios. For Maui, mean monthly fog-to-rainfall ratios were determined using the same general approach as Johnson and others (2018), but this study accounted for updates to (1) the assumed base altitude of the cloud zone in leeward areas and (2) the assumed top altitude of the cloud zone in all areas. One set of mean monthly fog-to-rainfall ratios was computed for each subarea as ratios of mean monthly potential fog interception to mean monthly rainfall (Giambelluca and others, 2013). For each calendar month, the mean monthly potential fog interception was assumed to equal the mean annual potential fog interception assigned to subareas according to fog regions (table 4; fig. 4) and prorated for each month according to the average number of days in the month. The mean monthly fog-to-rainfall ratios that were determined for Maui ensured that model estimates of mean annual fog interception for subareas with forest land-cover types in the baseline scenario would approximately equal the rates of potential fog interception (table 4), which were derived from fog-interception measurements in the Hawaiian Islands by Johnson and others (2018). Mean monthly fog-to-rainfall ratios were zero for all subareas below the cloud zones on Oʻahu and Maui.

Irrigation was estimated in the model only for subareas with selected agricultural land-cover type (coffee, diversified agriculture, pineapple, seed corn, and taro) or with selected developed land-cover type (golf course, high-intensity developed, and medium-intensity developed) that is assumed to contain irrigated lawns and landscapes. Supply-based irrigation rates and irrigation-specific model parameters (irrigation efficiency and irrigation multiplier) were not included in the sensitivity analysis because watershed management was assumed to have a limited effect on irrigation rates. Less than 0.4 percent of the combined area managed by watershed partnerships on Oʻahu and Maui was assigned a land-cover type with irrigation. Because taro was assumed to be grown in flooded pond fields, all subareas with taro land cover were assigned supply-based monthly irrigation rates that equaled the product of (1) the annual rate (455 inches per year) assigned to taro in recent model scenarios for Oʻahu and Maui (Engott and others 2017; Mair and others, 2019) and (2) the ratio of number of days in the month to number of days in the year. Irrigation rates for all remaining irrigated land covers on Oʻahu and Maui were estimated by the model using the demand-based approach and parameter values described by Engott and others (2017) and Mair and others (2019). Subareas on Oʻahu and Maui with a land-cover type of seed corn were assumed to consist of 75 percent seed corn and 25 percent bare soil by area, consistent with the assumption made by Engott and others (2017).

The spatial distributions of the ratio of the mean canopy evaporation rate during rainfall to mean precipitation rate for saturated canopy conditions ($\bar{E}/\bar{R}$), estimated by Engott and others (2017) for Oʻahu and by Johnson and others (2018) for Maui, were used for all model scenarios. Monthly ET_o values for each subarea were derived from maps of mean monthly ET_o obtained from Giambelluca and others (2014) and University of Hawaiʻi (2014a). Maps of daily and monthly ET_o were not available for the period used in the model simulations (1978–2007). Therefore, monthly ET_o values were not varied from year to year and were assumed to equal mean monthly ET_o values. For each subarea, ET_o was assumed to be the same each day of a given month. Engott and others (2017) and Mair and others (2019) estimated ET_o in the same manner.

Table 4. Rates of potential fog interception used to compute baseline fog-to-rainfall ratios used in model scenarios for the Island of Maui, Hawai‘i.

[Fog regions are at altitude and are listed in feet (ft) above local mean sea level; fog regions are shown in figure 4. Rates of potential fog interception were zero for areas not in fog regions. Abbreviation: in., inch]

Fog region (altitude above sea level)	Location relative to cloud zone	Mean annual potential fog interception (in.)
Leeward Maui between 2,600 and 7,800 ft	Within	14
Windward Maui between 2,000 and 7,800 ft	Within	30
Leeward Maui above 7,800 ft and below 9,000 ft	Above	10
Windward Maui above 7,800 ft and below 9,000 ft	Above	18
Maui 9,000 ft and above	Above	6

Representative available water capacity (AWC) values for soil horizons within the soil units on O‘ahu and Maui (NRCS 2019a, b) were used as model input with some modifications. The AWC values for the “rock land” soil unit were assigned to the (1) “rock outcrop” soil unit, which is consistent with modifications made by Engott and others (2017) and Mair and others (2019), and (2) the “quarry” soil unit, for which NRCS (2019a, b) did not provide AWC values. For Maui, AWC values for the “cinder land” and “stony alluvial land” soil units were assigned to the “cinder pit” and “gravel pit” soil units, respectively, because NRCS (2019a) did not provide AWC values for the “cinder pit” and “gravel pit” soil units. AWC values for O‘ahu and Maui were assumed to be no less than 0.01 inch of water per inch of soil.

The fraction of each subarea covered by built surfaces (fig. 3), which were considered impervious, was estimated using a GIS program. The impervious area of each subarea was determined in a GIS program by intersecting the subarea maps with maps of impervious surfaces for O‘ahu and Maui (National Oceanic and Atmospheric Administration, 2014, 2015). The built fraction of each subarea was computed as the ratio of (1) the impervious area of the subarea and (2) the total area of the subarea. However, the built fraction for subareas representing water bodies or reservoirs was assumed to be zero and the built fraction for the remaining subareas was assumed to be no greater than 0.99. Each subarea’s pervious fraction equaled 1 minus its built fraction.

Seepage from cesspools and other types of OSDSs was accounted for in the model simulations because O‘ahu and Maui contain more than 14,000 and 16,000 OSDSs, respectively (Whittier and El-Kadi, 2009, 2014). For the model calculations, seepage from cesspools was considered direct recharge whereas seepage from all other types of OSDSs was considered septic-system leachate (fig. 3). Model input with average daily rates of cesspool seepage and septic-system leachate for TMK parcels on O‘ahu and Maui were prepared from wastewater-discharge (effluent-flux) estimates in OSDS databases for O‘ahu and Maui (Hawai‘i State Department of Health, 2017). The O‘ahu and Maui OSDS databases, which are formatted as spatial datasets of points generally representing the centroids of TMK parcels that have OSDSs, included TMK numbers and effluent-flux estimates for the TMK parcels. For each O‘ahu TMK parcel, the cesspool seepage was assumed to equal the Class IV (cesspool) effluent flux shown in the O‘ahu OSDS database; septic-system leachate was assumed to equal the sum of effluent fluxes for the remaining OSDS classes shown in the O‘ahu OSDS database. The model inputs for Maui were prepared using a similar but different approach because the Maui OSDS database did not contain the same information as the O‘ahu OSDS database. For each Maui TMK parcel, cesspool seepage equaled the product of (1) the total effluent flux in the Maui OSDS database and (2) the ratio of the number of Class IV OSDSs to the total number of OSDSs in the Maui OSDS database. The septic-system leachate equaled the remainder of the effluent flux shown in the Maui OSDS database for the TMK parcel. For each model subarea within a TMK parcel that contains at least one OSDS, the average rates of cesspool seepage and septic-system leachate were converted from units of gallons per day to inches per day by assuming that (1) cesspool seepage was distributed as a uniform depth over the entire subarea and (2) septic-system leachate was distributed as a uniform depth over the subarea’s pervious area. The areas and spatial extents of TMK parcels were determined in a GIS program using maps of TMK parcels for O‘ahu (City and County of Honolulu, 2020) and Maui (Counties of Kaua‘i, Maui, and Hawai‘i, 2019). Cesspool seepage and septic-system leachate values for each of the dozens of TMK parcels not shown in the TMK maps were added to the corresponding values of the nearest TMK parcel included in the TMK maps. Recent applications of previous versions of the model (Engott and others, 2017; Mair and others, 2019) prepared model input using the same general approach but allowed only one type of effluent (cesspool seepage or septic-system leachate) in each TMK parcel.

Other Model Input Not Evaluated

Storm-drain capture (fig. 3), representing rainfall captured from built surfaces by storm-drain systems, was restricted to subareas with high- or medium-intensity developed land-cover types . The rejected-infiltration process was ignored by specifying an arbitrarily high soil infiltration capacity value (9,999 inches per day) to all subareas. For all model scenarios, the initial water storage of the built fraction of subareas was set to 0.125 in., equivalent to 50 percent of the rainfall-retention capacity value (0.25 in) assigned to built surfaces. The initial moisture storage of the pervious fraction of subareas was set at 50 percent of the soil moisture-storage capacity. The same initial values were used in recent water budgets for O‘ahu and Maui (Engott and others, 2017; Mair and others, 2019). To mitigate possible effects of the arbitrary initial values and random selection of monthly sets of daily-to-monthly rainfall ratios, each model scenario was run for 10 simulations and the results were averaged. Water seepage from reservoirs and other types of water bodies was treated as direct recharge (fig. 3) and was accounted for in the model scenarios using specified, constant recharge rates, which were the same as those specified by Engott and others (2017) for O‘ahu and by Mair and others (2019) for Maui. The model computed actual evapotranspiration before recharge for each simulated day.

Model Output

The model generated several output files for each scenario. The content of each output file is described by Oki (2022a). The sensitivity analysis selected each scenario’s output file that contained the mean annual water-budget components (in inches) that were averaged over all the scenario’s simulations, for each subarea. The modeled water-budget components in the selected output file included recharge as well as rainfall, fog interception, irrigation, septic-system leachate, direct recharge, run on from the built to unbuilt part of the subarea, canopy evaporation, net precipitation, storm-drain capture, and actual evapotranspiration derived from the plant-root zone exclusive of canopy evaporation. However, only the recharge values for subareas (Johnson and Kāne, 2023) were used in the sensitivity analysis.

Evaluation of Model Recharge Estimates for Sensitivity Analysis

The sensitivity of model recharge estimates to the selected parameters was evaluated for three moisture zones (dry, mesic, and wet) on O‘ahu and Maui (fig. 2). Price and others (2012) defined the moisture zones for the purpose of estimating the geographic ranges of plant species in the Hawaiian Islands. A map of the moisture zones for the Hawaiian Islands was created from a spatial dataset of the seven moisture subzones provided by Price and Jacobi (2012). Results of a sensitivity analysis were used to quantify the relative importance of each parameter on model recharge estimates for the dry, mesic, and wet moisture zones on O‘ahu and Maui only.

Computation of Parameter Sensitivity Indices for Moisture Zones

A numerical value, termed a parameter sensitivity index, was needed to determine the relative importance of a parameter for recharge assessment for each moisture zone. The model parameter values and corresponding recharge estimates for the subareas of O‘ahu and Maui were combined to form a pooled dataset that was then used to determine parameter sensitivity indices as follows. First, model recharge estimates for each subarea and scenario were converted from units of inches per year to million gallons per day. Next, the recharge for each moisture zone was computed for each scenario as the sum of the subarea recharge values, in million gallons per day, for the scenario. Next, an average parameter value was computed for each moisture zone and scenario, as follows:

$$P_{z,s} = \frac{\sum_{i=1}^{n} w_{i,z} p_{i,s}}{\sum_{i=1}^{n} w_{i,z}} \tag{1}$$

where

$P_{z,s}$ is the average parameter value for moisture zone z and scenario s associated with the parameter (table 3);

n is the number of subareas within moisture zone z;

$w_{i,z}$ is the area, in square meters, of subarea i within moisture zone z; and

$p_{i,s}$ is the parameter value assigned to subarea i for scenario s.

Next, an average baseline parameter value was computed for each moisture zone, as follows:

$$P_z = \frac{\sum_{i=1}^{n} w_{i,z}\, p_i}{\sum_{i=1}^{n} w_{i,z}} \tag{2}$$

where

P_z is the average baseline parameter value for moisture zone z; and

p_i is the baseline parameter value assigned to subarea i.

Next, pairs of explanatory ($\bar{P}_{z,s}$) and response ($\bar{R}_{z,s}$) values for each parameter were computed, as follows:

$$\bar{P}_{z,s} = \frac{P_{z,s}}{P_z} \times 100 \text{ percent, and} \tag{3}$$

$$\bar{R}_{z,s} = \frac{R_{z,s}}{R_z} \times 100 \text{ percent,} \tag{4}$$

where

$\bar{P}_{z,s}$ is the normalized average parameter value (and the explanatory value) for moisture zone z and scenario s associated with a parameter;

$\bar{R}_{z,s}$ is the normalized average recharge (and the response value) for moisture zone z and scenario s associated with a parameter;

$R_{z,s}$ is the sum of subarea recharge values for moisture zone z and scenario s associated with a parameter; and

R_z is the sum of baseline subarea recharge values for moisture zone z.

For each moisture zone and parameter, log-transformed explanatory values were computed as the natural logarithms of explanatory values. A parameter’s sensitivity index for a moisture zone was defined in this study as the slope of the line, determined using ordinary least squares regression (following Helsel and others, 2020), that either (1) related its response values to its log-transformed explanatory values (method 1) or (2) related its response values to its explanatory values (method 2). Scatter plots of response and explanatory values for both methods were examined and used to select one method for each moisture zone (table 5). Method 1 was selected for the dry and mesic moisture zones because scatter plots for the zones generally showed (1) a monotonic linear correlation between the log-transformed explanatory values

Table 5. Parameter sensitivity indices determined for moisture zones of the Islands of O‘ahu and Maui, Hawai‘i.

[Moisture zones shown in figure 2. A parameter's sensitivity index for a moisture zone represents the slope of the line, determined using ordinary least squares regression (Helsel and others, 2020), relating response values to explanatory values for the moisture zone and model scenarios associated with the parameter (figs. 5–7); Model recharge estimates for a moisture zone are more sensitive to a parameter whose sensitivity index is relatively far from zero compared with a parameter whose sensitivity index is closer to zero. Abbreviations: $\overline{P}$ values, normalized average parameter values for a moisture zone and model scenarios associated with a parameter; $\overline{R}$ values, normalized average recharge values for a moisture zone and model scenarios associated with a parameter. Pearson's *r* computed using method of Helsel and others (2020)]

Moisture zone	Explanatory and response values used to determine parameter sensitivity indices	Parameter sensitivity index (and Pearson's *r*)						
		Canopy capacity	Canopy-cover fraction	Crop coefficient	Fog-catch efficiency	Root depth	Stemflow	Trunk-storage capacity
Dry	$\overline{P}$ values transformed using natural logarithm and $\overline{R}$ values	−1.438 (−0.996)	−5.710 (−0.998)	−42.955 (−0.985)	1.839 (0.965)	−26.269 (−0.999)	−0.035 (−0.868)	−0.240 (−0.994)
Mesic	$\overline{P}$ values transformed using natural logarithm and $\overline{R}$ values	−13.477 (−0.996)	−17.303 (−0.998)	−68.032 (−1.000)	8.354 (0.970)	−12.729 (−0.999)	−0.365 (−0.884)	−1.424 (−0.999)
Wet	$\overline{P}$ values and $\overline{R}$ values	−0.091 (−0.998)	−0.115 (−0.998)	−0.203 (−1.000)	0.114 (1.000)	−0.005 (−0.942)	−0.001 (−0.599)	−0.008 (−0.969)

and response values for each parameter (figs. 5 and 6) and (2) a monotonic nonlinear correlation between the explanatory values and response values for some of the parameters. Method 2 was selected for the wet moisture zone because scatter plots for the zone generally showed a monotonic linear correlation between the explanatory values and response values for each parameter (fig. 7).

The use of more than one method to determine the parameter sensitivity indices was assumed to be acceptable because the sensitivity indices within each zone were computed using the same method, and comparisons of the sensitivity indices were constrained to one moisture zone at a time. This study did not compare the parameter sensitivity indices from one moisture zone with those from another moisture zone.

Summary of Parameter Sensitivity Indices for Moisture Zones

The parameter sensitivity indices for the moisture zone included positive and negative values (table 5). Fog-catch efficiency was the only parameter that had positive sensitivity indices, which indicates that recharge estimates for the moisture zones were directly proportional to the fog-catch-efficiency values—that is, recharge estimates increased and decreased when baseline fog-catch-efficiency values increased and decreased, respectively. Values of Pearson's *r* (Helsel and others, 2020) ranged from 0.965 to 1.000 across the three moisture zones for the sets of explanatory and response values selected for fog-catch efficiency. The remaining six parameters had negative sensitivity indices, which indicates that recharge estimates for the moisture zones were inversely proportional to the parameter values—that is, recharge estimates for the moisture zones increased and decreased when baseline parameters values decreased and increased, respectively. Values of Pearson's *r* ranged from −0.942 to −1.000 across the three moisture zones for the sets of explanatory and response values selected for canopy capacity, canopy-cover fraction, crop coefficient, root depth, and trunk-interception capacity. Values of Pearson's *r* ranged from −0.599 to −0.868 across the three moisture zones for stemflow, whose sensitivity indices were closer to zero than the other parameters and whose parameter values had relatively less effect on recharge values than the other parameters (figs. 5–7).

For each moisture zone, model recharge estimates were (1) less sensitive to parameters whose sensitivity indices were relatively close to zero and (2) more sensitive to parameters whose sensitivity indices were relatively far from zero (both positive and negative values). The sensitivity index for a given parameter and moisture zone can be used to estimate how much the moisture zone's normalized average recharge would be expected to change in response to a change to the zone's normalized average parameter value. For example, fog-catch efficiency had a sensitivity index of 0.114 for the wet moisture zone. Therefore, normalized recharge for the wet moisture zone would be expected to increase by 11.4 percent if the zone's normalized average baseline value for fog-catch efficiency increased by 100 percent. Or, alternatively, normalized recharge for the wet moisture zone would be expected to decrease by 1.14 percent if the zone's normalized average baseline fog-catch efficiency decreased by 10 percent.

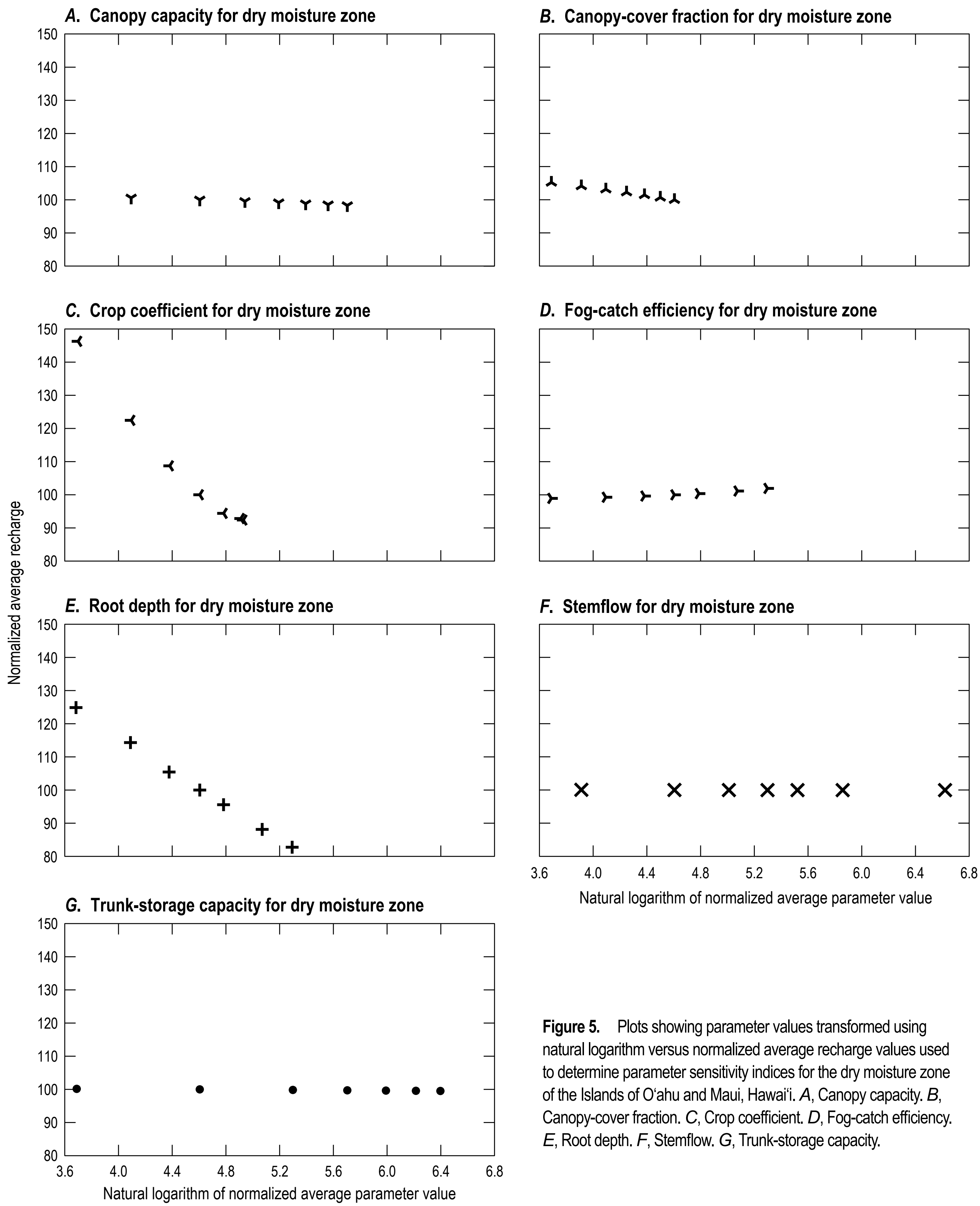

Figure 5. Plots showing parameter values transformed using natural logarithm versus normalized average recharge values used to determine parameter sensitivity indices for the dry moisture zone of the Islands of O‘ahu and Maui, Hawai‘i. *A*, Canopy capacity. *B*, Canopy-cover fraction. *C*, Crop coefficient. *D*, Fog-catch efficiency. *E*, Root depth. *F*, Stemflow. *G*, Trunk-storage capacity.

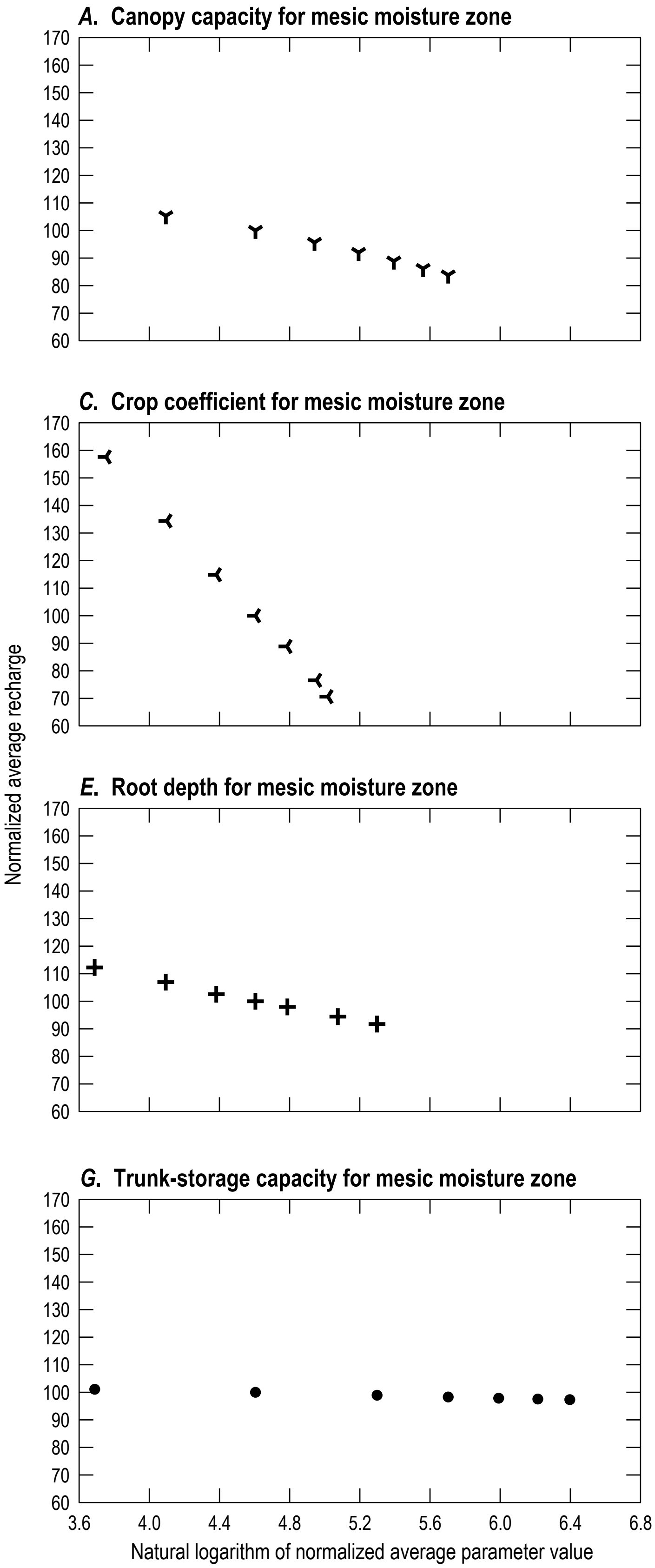

Figure 6. Plots showing parameter values transformed using natural logarithm versus normalized average recharge values used to determine parameter sensitivity indices for the mesic moisture zone of the Islands of O‘ahu and Maui, Hawai‘i. *A*, Canopy capacity. *B*, Canopy-cover fraction. *C*, Crop coefficient. *D*, Fog-catch efficiency. *E*, Root depth. *F*, Stemflow. *G*, Trunk-storage capacity.

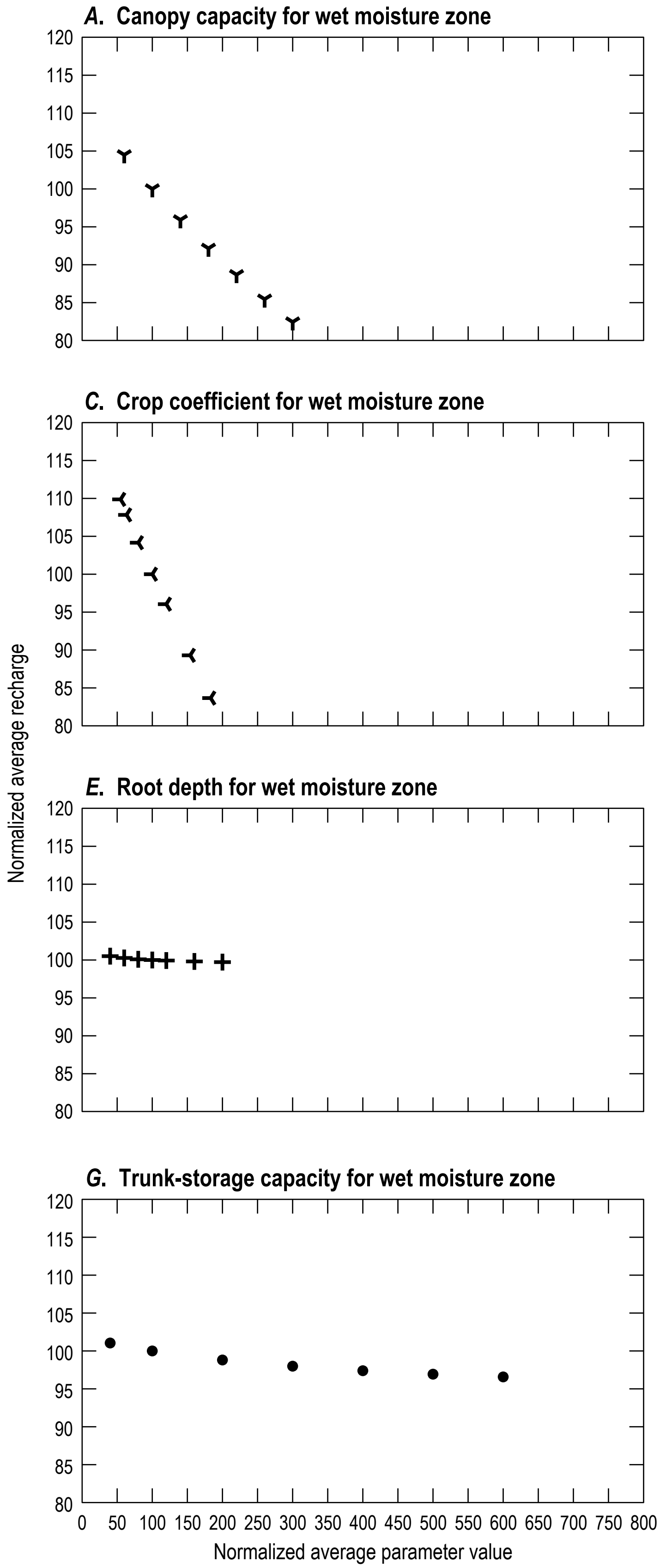

Figure 7. Plots showing parameter values versus normalized average recharge values used to determine parameter sensitivity indices for the wet moisture zone of the Islands of O‘ahu and Maui, Hawai‘i. *A*, Canopy capacity. *B*, Canopy-cover fraction. *C*, Crop coefficient. *D*, Fog-catch efficiency. *E*, Root depth. *F*, Stemflow. *G*, Trunk-storage capacity.

Relative Importance of Parameters to Recharge Assessment by Moisture Zone

A parameter's relative importance to recharge assessment for a moisture zone was determined on the basis of the parameter's sensitivity index for the zone (table 5) and the following equation:

$$I_z = \frac{A_z}{S_z} \times 100, \qquad (5)$$

where

I_z is the relative importance of the parameter to recharge assessment for moisture zone z;

A_z is the absolute value of the parameter's sensitivity index for moisture zone z; and

S_z is the sum of the absolute values of all parameter sensitivity indices for moisture zone z.

The relative importance of the parameters to recharge assessment within the moisture zones are presented in pie diagrams (fig. 8). Each moisture zone is represented by a pie diagram in which parameters with relatively large wedges are considered to be more important for assessing recharge relative to the parameters with relatively small wedges.

The method used to compute relative importance values (eq. 5) ensured that the sum of the relative importance values for each moisture zone equaled 100. Therefore, if one or more parameters had no effect on recharge estimates for a zone, then their relative importance values would be 0. If only one of the seven parameters affected recharge estimates for a zone, then its

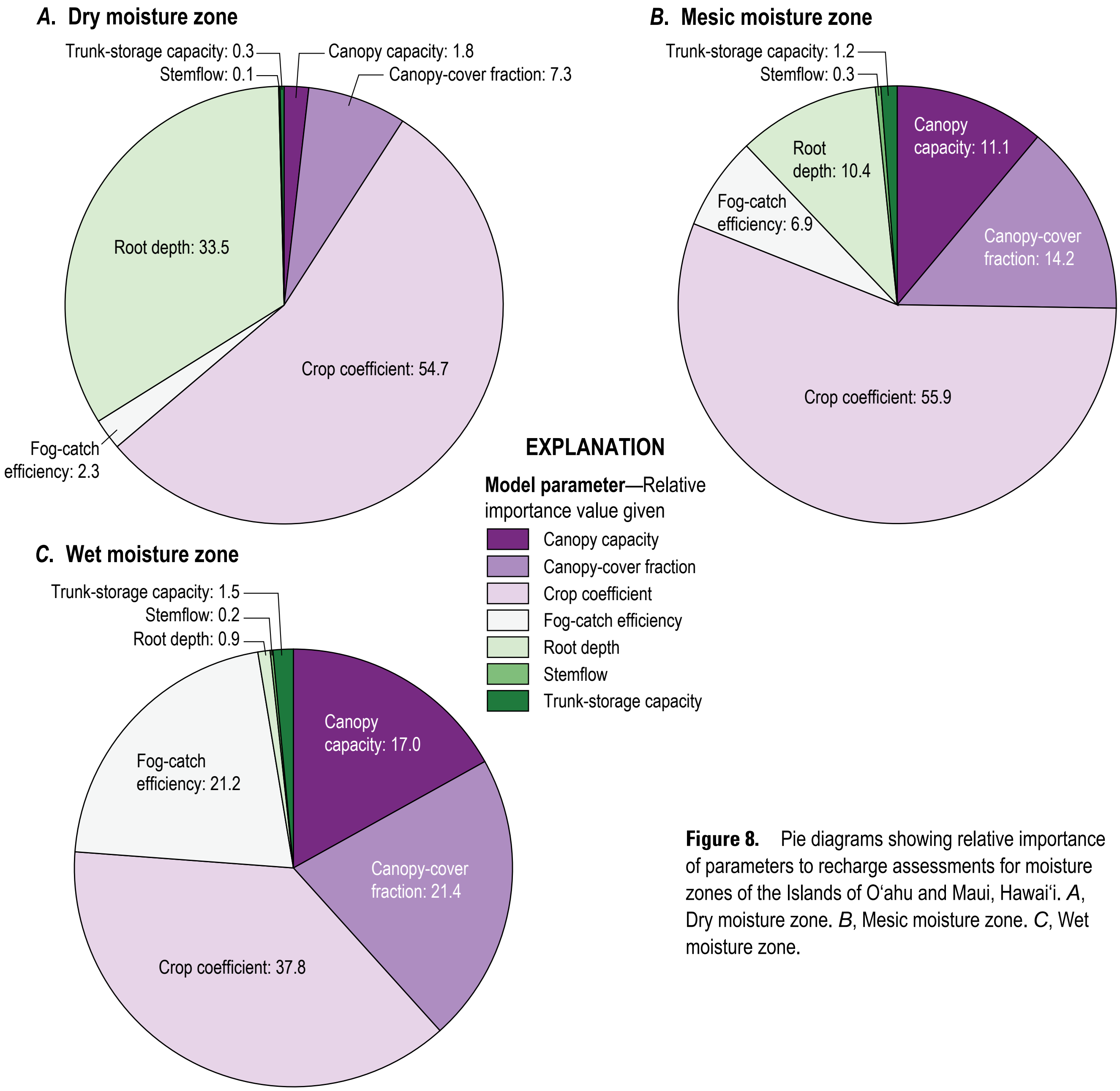

Figure 8. Pie diagrams showing relative importance of parameters to recharge assessments for moisture zones of the Islands of O'ahu and Maui, Hawai'i. *A*, Dry moisture zone. *B*, Mesic moisture zone. *C*, Wet moisture zone.

relative importance value would be 100. If all seven parameters had an equal effect on recharge estimates for a zone, then their relative importance values would be about 14.2 (that is, 100 divided by 7).

For the dry moisture zone, the crop-coefficient and root-depth parameters were the most important and had relative importance values (54.7 and 33.5, respectively) that were more than three times greater than the values for the other parameters. Canopy-cover fraction was the third most important parameter and had a relative importance value of 7.3. The remaining four parameters were less important and had relative importance values of 2.3 or less.

For the mesic moisture zone, crop coefficient was the most important parameter and had a relative importance value (55.9) that was more than two times greater than the values for the other parameters. Canopy-cover fraction, canopy capacity, and root depth were the next most important parameters and had similar relative importance values of 14.2, 11.1, and 10.4, respectively. The remaining three parameters were less important and had relative importance values of 6.9 or less.

For the wet moisture zone, crop coefficient was the most important parameter and had a relative importance value of 37.8. Canopy-cover fraction, fog-catch efficiency, and canopy capacity were the next most important parameters and had relative importance values of 21.4, 21.2, and 17.0, respectively. The remaining three parameters were less important and had relative importance values of 1.5 or less.

Information Needed to Quantify How Land-Cover Change Affects Recharge

Brief descriptions of the types of information needed to estimate values for each parameter are provided in table 6. Relative importance values of the parameters in table 6 can be used to prioritize collection of the most important types of data for the moisture zones.

The following list of critical information needs was created after an evaluation of the relative importance values and the types of data needed to estimate parameter values (table 6):

1. For all moisture zones, estimated rates of three evapotranspiration processes (ET_o, soil evaporation, and stand-level transpiration) are needed to estimate crop coefficients for
    - forests dominated by native trees and vegetation and
    - forests dominated by nonnative trees and vegetation.
2. For all moisture zones, estimated rates of two evapotranspiration processes (ET_o and total evapotranspiration) are needed to estimate crop coefficients for
    - shrubland vegetation and
    - grassland vegetation.

The estimation of total evapotranspiration rates for shrubland and grassland vegetation may require the estimation of soil evaporation, stand-level transpiration, and canopy evaporation, if appropriate.

1. For the dry and mesic moisture zones, estimates of average root depths are needed for
    - forests dominated by native trees and vegetation,
    - forests dominated by nonnative trees and vegetation,
    - shrubland vegetation, and
    - grassland vegetation.
2. For the wet and mesic moisture zones, estimates of canopy-cover fraction are needed for
    - forests dominated by native trees and vegetation and
    - forests dominated by nonnative trees and vegetation.
3. For the wet moisture zone, estimated rates of fog (cloud-water) interception are needed to estimate ratios of fog interception to rainfall for
    - forests dominated by native trees and vegetation,
    - forests dominated by nonnative trees and vegetation, and
    - shrubland vegetation
4. For the wet and mesic moisture zones, estimates of canopy capacity are needed for
    - forests dominated by native trees and vegetation and
    - forests dominated by nonnative trees and vegetation.

Forest, shrubland, and grassland were the only types of land cover considered here because they are the most common types of land cover in the collective area managed by watershed partnerships in the Hawaiian Islands and, therefore, the most likely to be affected by watershed management. Areas with forest, shrubland, and grassland land cover are estimated to make up about 46, 15, and 12 percent, respectively, of the collective area managed by the watershed partnerships. These coverage estimates were derived from (1) a spatial comparison of a watershed-partnership management area map (State of Hawaiʻi Department of Land and Natural Resources, 2018) with a map of existing vegetation lifeforms (U.S. Geological Survey, 2020) and (2) the assumption that forest, shrubland, and grassland were represented by the tree, shrub, and herb lifeforms, respectively.

In addition to the hydrologic information needs listed above, collection of information that reduces uncertainty of the baseline root-depth and crop-coefficient values assigned to sparsely vegetated land cover (table 2) is potentially important because this type of land cover is estimated to cover 24 percent of the collective area managed by watershed partnerships in the Hawaiian Islands and is especially widespread on the Island of Hawaiʻi. The other five parameters (canopy capacity, canopy-cover fraction, fog-catch efficiency, stemflow, and trunk-storage capacity) examined in the

Table 6. Types of hydrologic information needed to estimate parameter values and relative importance of seven model parameters to recharge assessment for moisture zones on the Islands of Oʻahu and Maui, Hawaiʻi.

[Moisture zones shown in figure 2. For each moisture zone, the sum of the relative importance values equals 100 and parameters that have larger relative importance values are more important to recharge assessment than parameters that have smaller relative importance values. Abbreviation: ET_o, reference grass surface evapotranspiration (Allen and others, 1998)]

Parameter	Relative importance by moisture zone			Information needed to estimate parameter values for different types of land cover
	Dry	Mesic	Wet	
Canopy capacity	1.8	11.1	17.0	Storage capacity of canopy for specific species or types of forest
Canopy-cover fraction	7.3	14.2	21.4	Fraction of ground area covered by vegetation for specific species or types of vegetation
Crop coefficient	54.7	55.9	37.8	Maximum stand-level transpiration and soil evaporation combined for forest areas; maximum stand-level total evapotranspiration (canopy evaporation, transpiration, and soil evaporation combined) for nonforest areas; ET_o for sites where transpiration, soil evaporation, and total evapotranspiration are estimated
Fog-catch efficiency	2.3	6.9	21.2	Rates of fog (cloud water) interception for specific species or types of vegetation; rainfall in the open near each fog-measurement site
Root depth	33.5	10.4	0.9	Average root depth for specific species or types of vegetation
Stemflow	0.1	0.3	0.2	Stemflow and precipitation (rainfall plus fog interception) for specific tree species or types of forests
Trunk-storage capacity	0.3	1.2	1.5	Storage capacity of tree trunks for specific tree species or types of forests

sensitivity analysis were assumed to have limited influence on recharge in areas with sparsely vegetated land cover. Other types of land cover represented by the remaining types of lifeforms (agricultural, developed, and water) were not considered because they are not widespread and, therefore, were assumed less likely to be broadly affected by watershed management.

Additional information collected within multiple moisture zones can be used to assess the accuracy of the simplified parameterization scheme used in the sensitivity analysis (table 2) and recent model applications for Oʻahu and Maui. The additional data may help future model users develop a better parameterization scheme that has moisture-zone and land-cover-specific parameter values, which would offer refinement over the general land-cover types used in the sensitivity analysis and recent model applications for Oʻahu and Maui. For example, data collected in native forests across multiple moisture zones could be used to determine separate crop coefficients for native forests within the dry, mesic, and wet moisture zones. Similarly, data collected in multiple moisture zones could be used to determine separate crop coefficients for nonnative forests, shrublands, and grasslands within each of the moisture zones.

Future model applications that attempt to quantify how recharge might be affected by species-specific types of land-cover changes may require values for important parameters (fig. 6) for the species of concern. For example, information could be collected to determine separate crop coefficients for forest stands dominated by different species of nonnative trees. High-priority nonnative species of concern for the Hawaiian Islands were identified during workshops held on Kauaʻi, Oʻahu, Maui, and the Island of Hawaiʻi in 2015 and 2018 and attended by representatives from CWRM, DOFAW, MDWS, UHM, The Nature Conservancy, watershed partnerships, other conservation groups and water utilities, and USGS (table 7). The identified nonnative species of concern were organized into five groups (three groups of tree species, one group of pasture and grassland species, and one group of shrub and substory species).

Recent applications of the model relied on temporally constant crop coefficients for forests, grassland, and shrubland vegetation. Temporally constant crop coefficients may not accurately represent evapotranspiration-related characteristics of selected types of vegetation, such as the nonnative tree *Fraxinus uhdei*, which is a winter deciduous species in the Hawaiian Islands and sheds its leaves every year (Harrington and Ewel, 1997). The collection of data that enables the estimation of monthly or seasonal crop coefficients for deciduous or other seasonally dependent vegetation could help improve the representation of these types of vegetation in the model.

Considerations for Estimation of Crop Coefficients

Crop coefficient was determined to be the most important parameter for all moisture zones (table 6). Measurements of three evapotranspiration processes (ET_o, soil evaporation, and stand-level transpiration) were identified as being required to estimate crop coefficients for forest vegetation. Measurements of two evapotranspiration processes (ET_o and stand-level total ET) were identified as being required to estimate crop coefficients for nonforest vegetation.

Several considerations related to evapotranspiration processes should be made prior to collecting evapotranspiration measurements. An estimated crop coefficient will have relatively low uncertainty if it is derived from measurements of all required evapotranspiration processes and if all required evapotranspiration processes were measured simultaneously at a study site. Conversely, an estimated crop coefficient will have

Table 7. Groups of high-priority nonnative species of concern for the Hawaiian Islands.

[The nonnative species of concern were identified by attendees at workshops held on the Islands of Kauaʻi, Oʻahu, Maui, and Hawaiʻi in 2015 and 2018. Workshop attendees included representatives from the County of Maui Department of Water Supply, Honolulu Board of Water Supply, County of Kauaʻi Department of Water Supply, County of Hawaiʻi Department of Water Supply, State of Hawaiʻi Commission on Water Resource Management, State of Hawaiʻi Division of Forestry and Wildlife, University of Hawaiʻi at Mānoa, The Nature Conservancy, watershed partnerships, Kauaʻi Invasive Species Committee, Maui Invasive Species Committee, Oʻahu Invasive Species Committee, Coordinating Group on Alien Pest Species, Oʻahu Army Natural Resources Program, U.S. Geological Survey Pacific Island Ecosystems Research Center, and U.S. Geological Survey Pacific Islands Water Science Center. Common name(s) of nonnative species selected from online databases including the Integrated Taxonomic Information System (https://www.itis.gov) and the Bishop Museum's Plants of Hawaiʻi (https://plantsofhawaii.org/).]

Common name(s) of nonnative species	Scientific name(s) of nonnative species
Group 1: Tree species identified on three or more islands	
Strawberry guava	*Psidium cattleianum*
Himalayan ginger	*Hedychium gardnerianum*
Albizia	*Falcataria moluccana*
Black wattle	*Acacia mearnsii*
Pine species (Monterey, Mexican weeping, maritime)	*Pinus radiata, P. patula, P. pinaster*
Tropical ash	*Fraxinus uhdei*
Christmas berry	*Schinus terebinthifolius*
Silk oak	*Grevillea robusta*
African tulip tree	*Spathodea campanulata*
Eucalyptus species (swamp mahogany, Sydney blue gum, Tasmanian blue gum)	*Eucalyptus robusta, E. saligna, E. globulus*
Ironwood	*Casuarina equisetifolia*
Firetree	*Morella faya*
Group 2: Tree species identified on two islands	
Gorse	*Ulex europaeus*
Java Plum	*Syzygium cumini*
Tree poppy	*Bocconia frutescens*
Banana poka	*Passiflora mollissima*
Group 3: Tree species identified on one island	
Australian red cedar	*Toona ciliata*
Paperbark tree	*Melaleuca quinquenervia*
Shoebutton ardisia	*Ardisia elliptica*
Kukui	*Aleurites moluccanus*
Octopus tree	*Schefflera actinophylla*
Koa haole	*Leucaena leucocephal*a
Group 4: Pasture and grassland species	
Guinea grass	*Megathyrsus maximus*
Buffelgrass	*Cenchrus ciliaris*
Broomsedge, broomsedge bluestem, yellow bluestem	*Andropogon virginicus*
Barbas de indio, West Indian foxtail	*Andropogon bicornis*
Bushy bluestem, bush beardgrass	*Andropogon glomeratus*
Columbian bluestem, little bluestem, tufted beardgrass	*Schizachyrium condensatum*
Fountain grass	*Cenchrus setaceus*
Kikuyu grass	*Cenchrus clandestinus*
Group 5: Shrub and substory species	
Koster's curse	*Clidemia hirta*
Australian tree fern	*Cyathea cooperi*
Miconia	*Miconia calvescens*
Yellow Himalayan raspberry	*Rubus ellipticus*
Hill raspberry, Mysore raspberry, snowpeaks raspberry	*Rubus niveus*
Latin American fleabane, daisy fleabane	*Erigeron karvinskianus*
Lantana	*Lantana camara*

relatively high uncertainty if it is derived from measurements of (1) only one required evapotranspiration process and assumed values for the remaining required evapotranspiration process(es) or (2) evapotranspiration processes that were not measured simultaneously at a study site. Furthermore, crop coefficients are likely to be underestimated if they are derived from estimates of evapotranspiration processes during periods when the evapotranspiration processes were restricted by shortage of available soil water, other evapotranspiration-limiting factors such as disease, grazing, or insect damage (Allen and others, 1998), or prolonged closure of leaf stomata (see, for example, Giambelluca and others, 2009). In contrast, crop coefficients are less likely to be underestimated if derived from estimates of evapotranspiration processes during periods when the evapotranspiration processes were not constrained by shortage of soil water or other evapotranspiration-limiting factors.

Future studies that examine existing forest stand-level transpiration estimates could aid in deriving crop coefficients for the different types of forests in the Hawaiian Islands (see, for example, Santiago and others, 2000; Giambelluca and others, 2003; Gaskill, 2004; Kagawa and others, 2009; Cavaleri and others, 2014; DeLay, 2015; Miyazawa and others, 2016; Dudley and others, 2020). Although all of those previous studies provided valuable information, the use of the information for crop-coefficient derivation is complicated by various study limitations. For example, many of the cited references reported average rates of stand-level transpiration for periods greater than a few months, during which transpiration might have been restricted by a shortage of soil water for all or part of the period. Also, none of the cited references reported rates of soil evaporation or ET_o for the same periods used to determine the reported stand-level transpiration rates. A few of the cited references, however, reported rates of *PE*—determined from the Penman (1948) or Penman-Monteith (Monteith, 1973) methods—which could be converted to rates of ET_o. In any case, the derivation of crop coefficients from the results of those cited references would require assumptions, such as an assumed soil-evaporation rate, an assumed ET_o rate, and an assumption of no soil-water stress during transpiration measurements—all of which would increase the uncertainty of the derived crop coefficients. However, the number of assumptions could potentially be reduced by an in-depth examination of the data collected for the aforementioned studies.

Study Limitations

The sensitivity analysis described in this report used a simple method, in which only one parameter was varied at time. The range of parameter values tested in the sensitivity scenarios for each parameter might not have included the entire parameter space (that is, the full range of parameter values), which is uncertain. The effect of these limitations could be examined by conducting a relatively complex, global sensitivity analysis that varies all parameters at a time and also considers variations within the entire parameter space (Pianosi and others, 2016), assuming that the parameter spaces can be ascertained.

This sensitivity analysis relied on rainfall and ET_o data (Giambelluca and others, 2013, 2014; Frazier and others, 2016) for recent climate conditions. The scope of the sensitivity analysis did not include use of climate-related data for projected future climate conditions (see, for example, Elison Timm and others, 2015; Zhang and others, 2016a, b; Elison Timm, 2017). The sensitivity analysis also did not consider the feasibility or cost of collecting water-budget information needed to reduce uncertainty of parameter values.

The sensitivity analysis did not include a model calibration step because recharge measurements were not available. The model cannot be calibrated to streamflow data recorded at streamgaging stations because WATRMod does not consider interactions between groundwater and surface water. The runoff-to-rainfall ratios used in the baseline scenario, however, ensured that model runoff estimates for drainage basins of selected streamgaging stations matched the runoff values that were estimated from the streamflow data of those streamgaging stations.

Each parameter value tested in the sensitivity scenarios was considered plausible. Model recharge estimates for subareas were considered plausible because the model balanced water inputs to the plant-soil system, water storage, and water outputs. The study did not attempt to determine the plausible range of recharge values for each subarea.

The model computed runoff as the product of rainfall and runoff-to-rainfall ratios. Consequently, the model's runoff computation method did not allow for consideration of parameters related to land-cover or forest-understory characteristics or processes. Therefore, runoff and runoff-to-rainfall ratios, which might be land-cover dependent, were not included in the sensitivity analysis. Sensitivity analyses completed for recent model applications indicated that runoff is an important factor controlling the water budget in the Hawaiian Islands (Engott and others, 2017; Izuka and others, 2018; Johnson and others, 2018; Oki and others, 2020). The hydrologic effect of watershed management on runoff, which is already recognized as an important information need, could be addressed separately using watershed modeling that was beyond the scope of this study. Additional limitations of the model and model input were described by Oki (2022a), Engott and others (2017), and Mair and others (2019).

Canopy evaporation was computed only for areas with forest land cover. The spatial extent of forest land cover in the model was defined from recent land-cover maps. Consequently, the model recharge estimates for nonforest areas were not affected by the values assigned to four parameters (canopy capacity, canopy-cover fraction, stemflow, and trunk-storage capacity) that were included in the sensitivity analysis and were needed to compute canopy evaporation. In contrast, values assigned to root depth and crop coefficient could have affected recharge in all forest and nonforest areas (other than water bodies and reservoirs). For example, if substantial areas of existing nonforest vegetation were to be replaced by forest vegetation in the future, then the relative importance values of the four forest-specific parameters might be greater than those estimated by this study.

Whereas both root depth and crop coefficient had the potential to affect recharge in all areas, the remaining five parameters (canopy capacity, canopy-cover fraction, fog-catch efficiency, stemflow, and trunk-storage capacity) only affected recharge in areas with some land covers.

Ratios of stemflow to precipitation (rainfall plus fog interception) tested in the sensitivity scenarios ranged from 0.02 to 0.3, which is less than the mean stemflow-to-rainfall ratio (0.34) reported by Safeeq and Fares (2014) for a nonnative forest site on O‘ahu dominated by Strawberry guava (*Psidium cattleianum*). The range of stemflow-to-precipitation ratios tested in the sensitivity scenarios do, however, span the range of monthly and annual stemflow-to-precipitation ratios (0.20–0.28) estimated for a nonnative forest site dominated by *P. cattleianum* on the Island of Hawai‘i by Takahashi and others (2011). Because the ratio of 0.34 was estimated for a site with no fog interception, its use in the model may overestimate stemflow in forests where rainfall is supplemented by fog interception. Therefore, a maximum value of 0.3 for the stemflow-to-precipitation ratios used in the sensitivity scenarios was considered appropriate.

For forest areas, the sum of canopy evaporation, transpiration, and soil evaporation might have occasionally exceeded *PE*. Therefore, total *ET* estimates for forested areas might have been overestimated given the amount of energy that was available for *ET*.

The relative importance of a parameter might have been underestimated if recharge was inversely proportional to the parameter’s values in some areas of a moisture zone but was directly proportional to the parameter’s values in other areas of the moisture zone. An examination of model recharge estimates for subareas indicated, however, that this phenomenon described in the preceding sentence was restricted to the scenarios for one parameter (crop coefficient) in two moistures zones (dry and mesic). Normalized recharge was inversely proportional to normalized average crop-coefficient values for both zones (figs. 5 and 6). Therefore, the relative importance of crop coefficient might have been underestimated for the two zones if recharge was directly proportional to crop-coefficient values for a substantial number of subareas in the two zones. An underestimation of crop coefficient’s relative importance would, however, have no effect on the list of information needs provided in this report because crop coefficient was the most important parameter in the two zones (table 6) (fig. 8). An examination of subarea recharge estimates indicated that recharge was directly proportional to crop coefficients for selected subareas with irrigation and whose combined area was only 2 percent of the dry moisture zone and only 0.2 percent of the mesic moisture zone. Because recharge was directly proportional to crop coefficient in only a minor percentage of each of the two zones, the phenomenon was assumed to have a minor effect on the relative-importance values determined for the two zones.

The model used in the sensitivity analysis has limitations. For example, the model cannot account for interactions between groundwater and surface water, and these interactions can be important in places such as streambeds. Throughout much of O‘ahu and Maui, however, the groundwater table is hundreds to thousands of feet below the land surface (Hunt, 1996; Izuka and others, 2018), and therefore, the extent of these interactions is not ubiquitous. Additional limitations of models that use a water-budget approach to estimate recharge for Hawaiian Islands are described by Engott and others (2017), Izuka and others (2018), Johnson and others (2018), Mair and others (2019), and Oki (2022a).

Summary

This report describes an evaluation of modeled recharge estimates and their sensitivity to seven model parameters that could be affected by land-cover changes associated with managed or unmanaged watersheds. Results of a sensitivity analysis were used to quantify the relative importance of each parameter on model recharge estimates for three moisture zones (dry, mesic, and wet) on the Hawaiian Islands of O‘ahu and Maui. Relative importance values for the parameters were used to prepare a list of critical information needs, which can guide future data-collection projects.

The identified critical information needs included estimates or measurements of (1) evapotranspiration processes needed to determine crop coefficients for forest, shrubland, and grassland types of land cover in all moisture zones, (2) rooting depths for forest, shrubland, and grassland types of land cover in the dry and mesic moisture zones, (3) canopy-cover fraction for forests in the wet and mesic moisture zones, (4) ratios of fog interception to rainfall for forests and shrublands in the wet moisture zone, and (5) canopy capacity for forests in the wet and mesic moisture zones. Collection and analysis of the identified critical information can be used to improve estimates of values assigned to important model parameters and reduce uncertainty of recharge estimates from future model applications that attempt to quantify how regional-scale recharge for the Hawaiian Islands might be affected by land-cover changes within a watershed.

References Cited

Allen, R.G., Pereira, L.S., Raes, D., and Smith, M., 1998, Crop evapotranspiration—Guidelines for computing crop water requirements: Food and Agriculture Organization of the United Nations, FAO Irrigation and Drainage Paper 56, 300 p., accessed June 9, 2011, at http://www.fao.org/docrep/X0490E/X0490E00.html.

Brewington, L., Keener, V., and Mair, A., 2019, Simulating land cover change impacts on groundwater recharge under selected climate projections, Maui, Hawai‘i: Remote Sensing, v. 11, no. 24, accessed April 2, 2021, at https://doi.org/10.3390/rs11243048.

Cavaleri, M.A., Ostertag, R., Cordell, S., and Sack, L., 2014, Native trees show conservative water use relative to invasive trees—Results from a removal experiment in a Hawaiian wet forest: Conservation Physiology, v. 2, no. 1, 14 p., accessed March 9, 2021, at https://doi.org/10.1093/conphys/cou016.

City and County of Honolulu, 2020, Parcel—Tax [originally published March 18, 2016]: City and County of Honolulu database, accessed February 13, 2020, at https://honolulu-cchnl.opendata.arcgis.com/datasets/.

Counties of Kaua‘i, Maui, and Hawai‘i, 2019, 015—Cadastral and Land Descriptions—TMK Parcels (All Islands), Neighbor Islands: State of Hawai‘i Office of Planning and Sustainable Development database, accessed February 25, 2020, at http://planning.hawaii.gov/gis/download-gis-data-expanded/.

DeLay, J.K., 2005, Canopy water balance on an elfin cloud forest at Alakahi, Hawai‘i: Honolulu, University of Hawai‘i, M.S. thesis, 78 p., accessed April 4, 2020, at https://hdl.handle.net/10125/11633.

DeLay, J.K., 2015, Forest transpiration on Kīlauea Volcano, Hawai‘i: Honolulu, University of Hawai‘i at Mānoa, Ph.D. dissertation, 130 p., accessed July 14, 2020, at https://hdl.handle.net/10125/51197.

DeLay, J.K., and Giambelluca, T.W., 2010, History of fog and cloud water interception research in Hawai‘i, *in* Bruijnzeel, L.A., Scatena, F.N., and Hamilton, L.S., eds., Tropical montane cloud forests—Science for conservation and management: New York, Cambridge University Press, p. 332–341.

Dudley, B.D., Hughes, R.F., Asner, G.P., Baldwin, J.A., Miyazawa, Y., Dulai, H., Waters, C., Bishop, J., Vaughn, N.R., Yeh, J., Kettwich, S., MacKenzie, R.A., Ostertag, R., and Giambelluca, T., 2020, Hydrological effects of tree invasion on a dry coastal Hawaiian ecosystem: Forest Ecology and Management, v. 458, no. 117653, 11 p., accessed June 19, 2020, at https://doi.org/10.1016/j.foreco.2019.117653.

Elison Timm, O., 2017, Future warming rates over the Hawaiian Islands based on elevation-dependent scaling factors: International Journal of Climatology, v. 37 (suppl. 1), p. 1093–1104, accessed October 3, 2017, at https://doi.org/10.1002/joc.5065.

Elison Timm, O., Giambelluca, T.W., and Diaz, H.F., 2015, Statistical downscaling of rainfall changes in Hawai‘i based on the CMIP5 global model projections: Journal of Geophysical Research— Atmospheres, v. 120, no. 1, p. 92–112, accessed October 16, 2017, at https://doi.org/10.1002/2014JD022059.

Engott, J.A., 2011, A water-budget model and assessment of groundwater recharge for the Island of Hawai‘i: U.S. Geological Survey Scientific Investigations Report 2011–5078, 53 p., accessed March 9, 2021, at https://doi.org/10.3133/sir20115078.

Engott, J.A., 2017, Mean annual water-budget components for the Island of O‘ahu, Hawaii, for average climate conditions, 1978-2007 rainfall and 2010 land cover (version 2.0): U.S. Geological Survey database, accessed October 2, 2020, at https://water.usgs.gov/GIS/metadata/usgswrd/XML/sir2015-5010_Oahu_WB_components_avg_climate.xml.

Engott, J.A., Johnson, A.G., Bassiouni, M., Izuka, S.K., and Rotzoll, K., 2017, Spatially distributed groundwater recharge for 2010 land cover estimated using a water-budget model for the Island of O‘ahu, Hawai‘i (ver. 2.0, December 2017): U.S. Geological Survey Scientific Investigations Report 2015–5010, 49 p., accessed February 6, 2020, at https://doi.org/10.3133/sir20155010.

Fares, A., 2013, Irrigation Water Requirement Estimation Decision Support System (IWREDSS) to estimate crop irrigation requirements for consumptive use permitting in Hawaii—Final report: Honolulu, Hawai‘i, University of Hawai‘i at Mānoa [prepared for State of Hawai‘i Department of Land and Natural Resources Commission of Water Resources Management], accessed August 28, 2020, at https://files.hawaii.gov/dlnr/cwrm/publishedreports/PR200808.pdf.

Finch, A.J., and Aronson, D.A., 1982, Water Resources Division publications guide—Volume 1. Publications policy and text preparation: U.S. Geological Survey Open-File Report 85–635, 497 p., accessed January 21, 2022, at https://doi.org/10.3133/ofr85635.

Frazier, A.G., Giambelluca, T.W., Diaz, H.F., and Needham, H.L., 2016, Comparison of geostatistical approaches to spatially interpolate month-year rainfall for the Hawaiian Islands: International Journal of Climatology, v. 36, no. 3, p. 1459–1470, accessed May 22, 2020, at https://doi.org/10.1002/joc.4437.

Gash, J.H.C., Lloyd, C.R., and Lachaud, G., 1995, Estimating sparse forest rainfall interception with an analytical model: Journal of Hydrology, v. 170, nos. 1–4, p 79–86, accessed March 9, 2021, at https://www.sciencedirect.com/science/article/pii/002216949502697N.

Gash, J.H.C., and Morton, A.J., 1978, An application of the Rutter model to the estimation of the interception loss from Thetford Forest: Journal of Hydrology, v. 38, nos. 1–2, p. 49–58, accessed March 9, 2021, at https://www.sciencedirect.com/science/article/pii/0022169478901312.

Gaskill, T.G.R., 2004, Hydrology of forest ecosystems in the Honouliuli Preserve—Implications for groundwater recharge and watershed restoration: Honolulu, University of Hawai‘i at Mānoa, Ph.D. dissertation, 177 p., accessed March 9, 2021, at https://hdl.handle.net/10125/12116.

Giambelluca, T.W., Chen, Q., Frazier, A.G., Price, J.P., Chen, Y.-L., Chu, P.-S., Eischeid, J.K., and Delparte, D.M., 2013, Online Rainfall Atlas of Hawai‘i: Bulletin of the American Meteorological Society, v. 94, no. 3, p. 313–316, accessed December 30, 2016, at https://doi.org/10.1175/BAMS-D-11-00228.1.

Giambelluca, T.W., DeLay, J.K., Nullet, M.A., Scholl, M.A., and Gingerich, S.B., 2011, Canopy water balance of windward and leeward Hawaiian cloud forests on Haleakalā, Maui, Hawai‘i: Hydrological Processes, v. 25, no. 3, p. 438–447, accessed April 1, 2020, at https://doi.org/10.1002/hyp.7738.

Giambelluca, T.W., Martin, R.E., Asner, G.P., Huang, M., Mudd, R.G., Nullet, M.A., DeLay, J.K., and Foote, D., 2009, Evapotanspiration and energy balance of native wet montane cloud forest in Hawai‘i: Agricultural and Forest Meteorology, v. 149, no. 2, p. 230–243, accessed February 18, 2021, at https://doi.org/10.1016/j.agrformet.2008.08.004.

Giambelluca, T.W., Shuai, X., Barnes, M.L., Alliss, R.J., Longman, R.J., Miura, T., Chen, Q., Frazier, A.G., Mudd, R.G., Cuo, L., and Businger, A.D., 2014, Evapotranspiration of Hawai‘i—Final report: Honolulu, University of Hawai‘i at Mānoa Department of Geography, submitted to the U.S. Army Corps of Engineers–Honolulu District, and the Commission on Water Resource Management, State of Hawai‘i, 78 p.

Giambelluca, T.W., Ziegler, A.D., Nullet, M.A., Truong, D.M., and Tran, L.T., 2003, Transpiration in a small tropical forest patch: Agricultural and Forest Meteorology, v. 117, nos. 1–2, p. 1–22, accessed March 9, 2021, at https://doi.org/10.1016/S0168-1923(03)00041-8.

Hamby, D.M., 1994, A review of techniques for parameter sensitivity analysis of environmental models: Environmental Monitoring and Assessment, v. 32, p. 135–154, accessed April 29, 2020, at https://doi.org/10.1007/BF00547132.

Harrington, R.A., and Ewel, J.J., 1997, Invasibility of tree plantations by native and non-indigenous plant species in Hawaii: Forestry Ecology and Management, v. 99, nos. 1–2, p. 153–162, accessed March 15, 2021, at https://doi.org/10.1016/S0378-1127(97)00201-6.

Hawai‘i State Department of Health, 2017, 019—Utilities and networks—On-site sewage disposal systems (OSDS), O‘ahu (2008) and Maui (2010): State of Hawai‘i Office of Planning and Sustainable Development database, accessed February 27, 2020, at https://planning.hawaii.gov/gis/download-gis-data-expanded.

Helsel, D.R., Hirsch, R.M., Ryberg, K.R., Archfield, S.A., and Gilroy, E.J., 2020, Statistical methods in water resources: U.S. Geological Survey Techniques and Methods, book 4, chap. A3, 458 p., accessed June 25, 2020, at https://doi.org/10.3133/tm4a3.

Hunt, C.D., Jr., 1996, Geohydrology of the Island of Oahu, Hawaii: U.S. Geological Survey Professional Paper 1412–B, 54 p., accessed October 28, 2021, at https://doi.org/10.3133/pp1412B.

Izuka, S.K., Engott, J.A., Rotzoll, K., Bassiouni, M., Johnson, A.G., Miller, L.D., and Mair, A., 2018, Volcanic aquifers of Hawai‘i—Hydrogeology, water budgets, and conceptual models (ver. 2.0, March 2018): U.S. Geological Survey Scientific Investigations Report 2015–5164, 158 p., accessed November 16, 2018, at https://doi.org/10.3133/sir20155164.

Johnson, A.G., Engott, J.A., Bassiouni, M., and Rotzoll, K., 2018, Spatially distributed groundwater recharge estimated using a water-budget model for the Island of Maui, Hawai‘i, 1978–2007 (ver. 2.0, February 2018): U.S. Geological Survey Scientific Investigations Report 2014–5168, 53 p., accessed April 2, 2020, at https://doi.org/10.3133/sir20145168.

Johnson, A.G., and Kāne, H.L, 2023, Model subareas and moisture zones used in a sensitivity analysis of a water-budget model completed in 2022 for the islands of Oahu and Maui, Hawaii: U.S. Geological Survey data release, accessed at https://doi.org/10.5066/P9X9ZEE3.

Juvik, J.O., DeLay, J.K., Kinney, K.M., and Hansen, E.W., 2011, A 50th anniversary reassessment of the seminal ‘Lāna‘i fog drip study’ in Hawai‘i: Hydrologic Processes v. 25, no. 3, accessed March 25, 2020, at https://doi.org/10.1002/hyp.7803.

Juvik, J.O., and Hughes, K., 1997, Climatology and water resources at Kahikinui, Maui, Final Report—1997: Hilo, Hawai‘i, Pacific Environmental Planning, 24 p.

Kagawa, A., Sack, L., Duarte, K., and James, S., 2009, Hawaiian native forest conserves water relative to timber plantation—Species and stand traits influence water use: Ecological Applications, v. 19, no. 6, p. 1429–1443, accessed March 9, 2021, at https://doi.org/10.1890/08-1704.1.

Longman, R.J., Frazier, A.G., Newman, A.J., Giambelluca, T.W., Schanzenbach, D., Kagawa-Viviani, A., Needham, H., Arnold, J.R., and Clark, M.P., 2019, High-resolution gridded daily rainfall and temperature for the Hawaiian Islands (1990–2014): Journal of Hydrometeorology, v. 20, no. 3, p. 489–508, accessed March 10, 2020, at https://doi.org/10.1175/JHM-D-18-0112.1.

Mair, A., 2018, Land-cover map for the Island of Maui, Hawaii, 2017 (ver. 1.2, November 2018): U.S. Geological Survey data release, accessed November 30, 2018, at https://doi.org/10.5066/F7DF6PPB.

Mair, A., and Fares, A., 2010, Throughfall characteristics in three non-native Hawaiian forest stands: Agricultural and Forest Meteorology, v. 150, no. 11, p. 1453–1466, accessed March 12, 2021, at https://doi.org/10.1016/j.agrformet.2010.07.007.

Mair, A., Johnson A.G., Rotzoll, K., and Oki, D.S., 2019, Estimated groundwater recharge from a water-budget model incorporating selected climate projections, Island of Maui, Hawai‘i: U.S. Geological Survey Scientific Investigations Report 2019–5064, 46 p., accessed August 23, 2019, at https://doi.org/10.3133/sir20195064.

McJannet, D., Wallace, J., Fitch, P., Disher, M., and Reddell, P., 2007, Water balance of tropical rainforest canopies in north Queensland, Australia: Hydrological Processes, v. 21, no. 25, p. 3473–3484, accessed April 2, 2021, at https://doi.org/10.1002/hyp.6618.

Miyazawa, Y., Dudley, B.D., Hughes, R.F., Vandemark, J., Cordell, S., Nullet, M.A., Ostertag, R., and Giambelluca, T.W., 2016, Non-native tree in a dry coastal area in Hawai‘i has high transpiration but restricts water use despite phreatophytic trait: Ecohydrology, v. 9, no. 7, p. 1166–1176, accessed March, 9, 2021, at https://doi.org/10.1002/eco.1715.

Monteith, J.L., 1973, Principles of Environmental Physics: London, Edward Arnold, 241 p.

National Gap Analysis Program, 2011, Land cover data download—Hawaii (ver. 2): U.S. Geological Survey database, accessed March 18, 2020, at https://www.usgs.gov/core-science-systems/science-analytics-and-synthesis/gap/science/land-cover-data-download.

National Oceanic and Atmospheric Administration, 2014, C-CAP high-resolution land cover and change—2011 NOAA high res land cover—HI Oahu: National Oceanic and Atmospheric Administration, Office for Coastal Management, Digital Coast database, accessed October 5, 2020, at https://coast.noaa.gov/digitalcoast/data/ccaphighres.html.

National Oceanic and Atmospheric Administration, 2015, C-CAP high-resolution land cover and change—2010 NOAA high res land cover—HI Maui: National Oceanic and Atmospheric Administration, Office for Coastal Management, Digital Coast database, accessed October 5, 2020, at https://coast.noaa.gov/digitalcoast/data/ccaphighres.html.

Natural Resources Conservation Service [NRCS], 2019a, Web soil survey—Soil survey geographic (SSURGO) database for the Island of Maui: U.S. Department of Agriculture, Natural Resources Conservation Service database, accessed December 5, 2019, at https://websoilsurvey.nrcs.usda.gov/app/WebSoilSurvey.aspx.

Natural Resources Conservation Service [NRCS], 2019b, Web soil survey—Soil survey geographic (SSURGO) database for the Island of Oahu: U.S. Department of Agriculture, Natural Resources Conservation Service database, accessed December 5, 2019, at https://websoilsurvey.nrcs.usda.gov/app/WebSoilSurvey.aspx.

Oki, D.S., 2022a, Water-budget accounting for tropical regions model (WATRMod) documentation: U.S. Geological Survey Open-File Report 2021–1013, 71 p., accessed August 2, 2022, at https://doi.org/10.3133/ofr20221013.

Oki, D.S., 2022b, WATRMod, a water-budget accounting for tropical regions model—Source code, executable file, and example files: U.S. Geological Survey data release, accessed August 2, 2022, at https://doi.org/10.5066/P9VPAY41.

Oki, D.S., Engott, J.A., and Rotzoll, K., 2020, Numerical simulation of groundwater availability in central Moloka‘i, Hawai‘i: U.S. Geological Survey Scientific Investigations Report 2019–5150, 95 p., accessed May 26, 2020, at https://doi.org/10.3133/sir20195150.

Oki, D.S., Wolff, R.H., and Perreault, J.A., 2010, Effects of surface-water diversion on streamflow, recharge, physical habitat, and temperature, Nā Wai ‘Ehā, Maui, Hawai‘i: U.S. Geological Survey Scientific Investigations Report 2010–5011, 154 p., accessed April 7, 2021, at https://doi.org/10.3133/sir20105011.

Penman, H.L., 1948, Natural evaporation from open water, bare soil and grass: Proceedings of the Royal Society A, v. 193, no. 1032, p. 120–146, accessed September 15, 2023, at https://doi.org/10.1098/rspa.1948.0037.

Pianosi, F., Beven, K., Freer, J., Hall, J.W., Rougier, J., Stephenson, D.B., and Wagener, T., 2016, Sensitivity analysis of environmental models—A systematic review with practical workflow: Environmental Modelling & Software, v. 79, p. 214–232, accessed April 30, 2020, at https://doi.org/10.1016/j.envsoft.2016.02.008.

Price, J.P., and Jacobi, J.D., 2012, Moisture zones for the main Hawaiian Islands: U.S. Geological Survey data release, accessed January 8, 2021, at https://www.sciencebase.gov/catalog/item/57a902e8e4b05e859bdf3c83.

Price, J.P., Jacobi, J.D., Gon, S.M., III, Matsuwaki, D., Mehrhoff, L., Wagner, W., Lucas, M., and Rowe, B., 2012, Mapping plant species ranges in the Hawaiian Islands—Developing a methodology and associated GIS layers: U.S. Geological Survey Open-File Report 2012–1192, 34 p., 1 appendix, 1,158 maps, accessed January 8, 2021, at https://doi.org/10.3133/ofr20121192.

Safeeq, M., and Fares, A., 2014, Interception losses in three non-native Hawaiian forest stands: Hydrological Processes, v. 28, no. 2, p. 237–254, accessed July 2, 2020, at https://doi.org/10.1002/hyp.9557.

Santiago, L.S., Goldstein, G., Meinzer, F.C., Fownes, J.H., and Mueller-Dombois, D., 2000, Transpiration and forest structure in relation to soil waterlogging in a Hawaiian montane cloud forest: Tree Physiology, v. 20, no. 10, p. 673–681, accessed March 9, 2021, at https://doi.org/10.1093/treephys/20.10.673.

Schenk, H.J., and Jackson, R.B., 2002, The global biogeography of roots: Ecological Monographs, v. 72, no. 3, p. 311–328, accessed November 9, 2020, at https://doi.org/10.1890/0012-9615(2002)072[0311:TGBOR]2.0.CO;2.

State of Hawai‘i Department of Land and Natural Resources, 2011, The rain follows the forest—A plan to replenish Hawaii’s source of water: State of Hawai‘i Department of Land and Natural Resources, 21 p.

State of Hawai‘i Department of Land and Natural Resources, 2018, 003—Administrative and political boundaries—Watershed partnerships: State of Hawai‘i Office of Planning and Sustainable Development database, accessed August 3, 2020, at https://planning.hawaii.gov/gis/download-gis-data-expanded/.

Takahashi, M., Giambelluca, T.W., Mudd, R.G., DeLay, J.K., Nullet, M.A., and Asner, G.P., 2011, Rainfall partitioning and cloud water interception in native forest and invaded forest in Hawai‘i Volcanoes National Park: Hydrological Processes, v. 25, p. 448–464, accessed April 23, 2020, at https://doi.org/10.1002/hyp.7797.

University of Hawai‘i, 2014a, Evapotranspiration of Hawai‘i—Grass reference surface potential evapotranspiration: Honolulu, University of Hawai‘i at Mānoa Geography Department database, accessed August 2, 2019, at http://evapotranspiration.geography.hawaii.edu/downloads.html.

University of Hawai‘i, 2014b, Evapotranspiration of Hawai‘i—Vegetation cover fraction: Honolulu, University of Hawai‘i at Mānoa Geography Department database, accessed August 2, 2019, at http://evapotranspiration.geography.hawaii.edu/downloads.html.

University of Hawai‘i, 2015, Rainfall atlas of Hawai‘i—Month-year rainfall maps for the State of Hawai‘i: Honolulu, University of Hawai‘i at Mānoa Geography Department database, accessed January 25, 2017, at http://rainfall.geography.hawaii.edu/downloads.html.

U.S. Geological Survey, 2020, LANDFIRE—LF 2016 Remap [LF 2.0.0]—Existing vegetation type (EVT), Hawai‘i: U.S. Geological Survey database, accessed January 11, 2021, at https://www.landfire.gov/version_comparison.php.

Whittier, R.B., and El-Kadi, A.I., 2009, Human and environmental risk ranking of onsite sewage disposal systems for Oahu: Honolulu, University of Hawai‘i at Mānoa [prepared for Hawai‘i Department of Health Safe Drinking Water Branch], 142 p., accessed February 13, 2020, at https://hdl.handle.net/10125/50770.

Whittier, R.B., and El-Kadi, A.I., 2014, Human and environmental risk ranking of onsite sewage disposal systems for the Hawaiian islands of Kauai, Molokai, Maui, and Hawaii: Honolulu, University of Hawai‘i at Mānoa [prepared for Hawai‘i Department of Health Safe Drinking Water Branch], 257 p., accessed February 13, 2020, at https://hdl.handle.net/10125/50771.

Yang, Y., Donohue, R.J., and McVicar, T.R., 2016, Global estimation of effective plant rooting depth—Implications for hydrologic modeling: Water Resources Research, v. 52, no. 10, p. 8260–8276, accessed November 9, 2020, at https://doi.org/10.1002/2016WR019392.

Zhang, C., Wang, Y., Hamilton, K., and Lauer, A., 2016a, Dynamical downscaling of the climate for the Hawaiian Islands, Part I—Present day: Journal of Climate, v. 29, no. 8, p. 3027–3048, accessed May 16, 2016, at https://doi.org/10.1175/JCLI-D-15-0432.1.

Zhang, C., Wang, Y., Hamilton, K., and Lauer, A., 2016b, Dynamical downscaling of the climate for the Hawaiian Islands, Part II—Projection for the late twenty-first century: Journal of Climate, v. 29, no. 23, p. 8333–8354, accessed April 6, 2017, at https://doi.org/10.1175/JCLI-D-16-0038.1.

Zhang, C., Wang, Y., Lauer, A., Hamilton, K., and Xie, F., 2012, Cloud base and top heights in the Hawaiian region determined with satellite and ground-based measurements: Geophysical Research Letters, v. 39, no. 15, 6 p., accessed December 3, 2020, at https://doi.org/10.1029/2012GL052355.

Moffett Field Publishing Service Center
Manuscript approved February 19, 2023
Edited by Kathryn Pauls
Illustration support by Katie Sullivan
Layout by Cory Hurd

Johnson and others—**Identifying the Relative Importance of Water-Budget Information, Hawaiian Islands**—Scientific Investigations Report 2023–5022

ISSN 2328-0328 (online)
https://doi.org/10.3133/sir20235022